1   # Cold sensitivity of the SARS-CoV-2 spike ectodomain

2

3   Robert J Edwards[1,2‡,*], Katayoun Mansouri[1,‡], Victoria Stalls[1,‡], Kartik Manne[1, ‡],

4   Brian Watts[1], Rob Parks[1], Katarzyna Janowska[1], Sophie M. C. Gobeil[1], Megan Kopp[1], Dapeng

5   Li[1], Xiaozhi Lu[1], Zekun Mu[1], Margaret Deyton[1], Thomas H Oguin III[1], Jordan Sprenz[1], Wilton

6   Williams[1,2], Kevin Saunders[1,3], David Montefiori[1,3], Gregory D. Sempowski[1], Rory Henderson[1,2],

7   Munir Alam[1,2], Barton F. Haynes[1,2], Priyamvada Acharya[1,3,*]

8

9   **Affiliations:**
10   [1] Duke Human Vaccine Institute, Durham NC 27710, USA
11   [2] Duke University, Department of Medicine, Durham NC 27710, USA
12   [3] Duke University, Department of Surgery, Durham NC 27710, USA
13   [4] Duke University, Department of Immunology, Durham NC 27710, USA
14   ‡These authors contributed equally.
15   *To whom correspondence should be addressed
16
17   Correspondence to: Robert J Edwards (rj.edwards@duke.edu) and Priyamvada Acharya
18   (priyamvada.acharya@duke.edu)

19

20

21

22

23

24

25

26

27

28

Abstract

30   The SARS-CoV-2 spike (S) protein, a primary target for COVID-19 vaccine development,

31   presents its Receptor Binding Domain in two conformations: receptor-accessible "up" or

32   receptor-inaccessible "down" conformations. Here, we report that the commonly used stabilized

33   S ectodomain construct "2P" is sensitive to cold temperature, and that this cold sensitivity is

34   resolved in a "down" state stabilized spike. Our results will impact structural, functional and

35   vaccine studies that use the SARS-CoV-2 S ectodomain.

36
37
38
39
40
41
42
43

44   The spike (S) protein of SARS-CoV-2 mediates receptor binding and cell entry and is a

45   key target for vaccine development efforts. Stabilized S ectodomain constructs have been

46   developed that mimic the native spike, bind ACE-2 receptor [1,2], and present epitopes for

47   neutralizing antibodies on their surface [3-6]. The "2P" S-ectodomain construct examined here

48   incorporates residues 1-1208 of the SARS-CoV-2 spike, with two proline mutations in C-terminal

49   S2 domain designed to stabilize the pre-fusion spike conformation, a C-terminal foldon

50   trimerization motif, and a mutation that abrogates the furin cleavage site [1] (Figure 1a). This and

51   similar constructs are being widely used for structural biology and vaccine studies [1-3,7,8]. Purified

52   S ectodomain proteins [9] are assessed for quality control by SDS-PAGE, size exclusion

53   chromatography (SEC), differential scanning fluorimetry (DSF) [10], and negative stain electron

54   microscopy (NSEM). NSEM has proved especially important because it reveals the three-

55   dimensional structural integrity of individual molecules, allowing us to discriminate between

56   preparations that looked similar by bulk methods such as SDS-PAGE and SEC (Extended Data

57   Figure 1). The observed variability in the spike fraction between preparations suggests a fragile

58   S ectodomain, and measures to overcome the issue have been previously reported [11,12]. Here

59   we link the apparent fragility of spike ectodomain 2P to its rapid denaturation upon storage at 4

60   °C (Figure 1 b-e).

61   We followed the structural, biophysical and antigenic features of the S ectodomain

62   stored under different temperatures conditions (Figure 1, Extended Data Figures 2-6). The 2P

63   spike was produced in 293F cells at 37 °C and the purification was performed at room

64   temperature and completed within 6-8 hours (Supplementary Figure 1a-c) . Representative

65   NSEM micrographs obtained of the 2P spike incubated at different temperatures and shown

66   (Figure 1b-d, Supplementary Figure 1d-e) , and results summarized in Figure 1e. Freshly

67   prepared spike samples assessed on the same day they were purified showed 75% well-formed

68   spikes on average (Fig 1b,e); this fraction slightly decreased to 64% after one cycle of

69   freeze/thaw and to 59% by storage at room temperature (22 ºC) for 5–7 days (Supplementary

70   Figure 1d,e); and it was substantially reduced to 5% after storage at 4 ºC for 5–7 days (Fig

71   1c,e). In contrast, after 1-week storage at 37 °C, we observed 83% well-formed spike.

72   Furthermore, well-formed spike could be recovered after the spike was stored at 4 °C for a week

73   with a 3-hour incubation at 37 °C to ~75% (Figure 1d,e); no further improvement was observed

74   after longer incubations at 37 °C (Figure 1e) which actually led to slight aggregation

75   (Supplemental Figure 1e). SDS-PAGE analysis (Supplementary Figure 1) of 2P spike samples

76   stored at different temperatures does not indicate any appreciable degradation of the spike,

77   although we do observe evidence of higher molecular weight species in spike stored at 37 °C

78   for a week (Supplemental Figure 1). Similar to our NSEM results, we also see substantial

79   differences in the quality and dispersion of protein in cryo-EM grids depending on the

80   temperature the specimen was stored (Extended Data Figure 6). In summary, these data show

81   that the 2P spike denatured upon storage for at 4 °C for a week, and this denaturation could be

82   at least partially reversed by incubating the sample at 37 °C following cold-storage.

83   The S ectodomain was reported to exhibit conformational changes in response to pH[12],

84   so we asked whether the spike denaturation observed was due to temperature-dependent pH

85   changes at 4 °C in the Tris pH 8.0 buffer we used[13] . A Tris buffer solution that measures pH 8.0

86   at 25 °C would measure ~pH 8.6 at 4 °C. We performed SEC purification of a 2P spike

87   preparation into MOPS buffer pH 7.4. MOPS has a smaller temperature dependence compared

88   to Tris[13], and is expected to change only slightly to pH 7.42 at 4 °C . Cold-storage at pH 7.42

89   (MOPS buffer) reduced the spike fraction to 4%, similar to the average of 5% for cold-storage in

90   Tris buffer (Figure 1e). Thus, the primary cause of spike denaturation appears to be the

91   temperature change and not the pH shift within this range. We also tested the temperature

92   effect at acidic pH and found that incubating the spike at 4 °C in MES, pH 6 buffer reduced but

93   did not eliminate the cold-sensitivity (Fig 1e).

94   We next examined whether the observed cold sensitivity is a property of the bulk protein

95   in solution, rather than an artifact of the NSEM sample preparation. First, we used a rapid DSF

96   assay[10] that measures changes in the intrinsic fluorescence of the protein as a thermal ramp is

97   applied. The changes in fluorescence signal indicate transitions in the folding state of a protein,

98   the temperature at which a transition occurs is called the inflection temperature (Ti). Distinct

99   profile shifts were observed for spike samples stored at different temperatures, with Ti shifted

100   toward lower temperatures for spike samples stored at 4 °C, indicating lower protein stability,

101   compared to when the spike was stored at 22 °C or 37 °C (Figures 1f). Next, we measured

102   melting temperatures (T_m) using differential scanning calorimetry (DSC) (Figure 1g and

103   Extended Data Figure 3): after one-week storage at 37 °C, the spike sample featured an

104   asymmetric unfolding transition with T_m of 65.5 °C. After one-week storage at 22 °C, we

105   observed a second low-T_m transition at 48.2 °C. After one-week storage at 4°C, we observed a

106   similar two-peak profile with a markedly more pronounced low-T_m transition (T_m = 48.4 °C).

107   Upon returning the 4 °C sample to 37 °C for 3 hours prior to analysis, we observed an amplitude

108   reduction of the low-T_m transition (T_m = 49.2 °C) and a corresponding amplitude increase in the

109   high-T_m transition (T_m = 66.0 °C). Thus, the DSC results confirm that storage at 4 °C

110   destabilizes the spike compared to samples stored at 22 °C or 37 °C, and that returning the

111   destabilized spike to 37 °C for 3 hours substantially restores its stability, although the presence

112   of the low-Tm peak suggests that the recovery is partial.

113   We next tested the effects of cold-induced spike instability on antibody and receptor

114   binding by SPR and ELISA (Figures 1h and Extended Data Figures 4-5, Supplementary Figure

115   2). We found that spike stored at 4 °C showed higher binding to antibody CR3022 (Figure 1h,

116   Extended Data Figure 4, Supplementary Figure 2) and the receptor ACE-2 (Extended Data

117   Figure 4), which both require an "up" RBD conformation for stable binding[1,9,12]. In contrast, cold-

118   storage reduced binding to antibody 2G12 (Figure 1h, Extended Data Figure 4, Supplementary

119   Figure 2), which recognizes a quaternary glycan epitope in the S2 subunit[14] indicating loss of

120   quaternary structure during cold storage. We also tested two antibodies isolated from a COVID-

121   19 convalescent donor (Supplementary Figures 4-5), with epitopes mapped to the ACE-2

122   binding site (AB712199) and to the S2 region of the spike (AB511584) (Supplementary Figure

123   4). Both antibodies showed different binding profiles depending on the temperature at which the

124   spike was stored, highlighting the importance of accounting for this cold-sensitive behavior of

125   the S ectodomain for obtaining consistent results in serology assays when using the 2P spike or

126   similar constructs. We next tested CR3022 and 2G12 binding to freshly prepared 2P spike

127   sample and compared it to a sample that was flash frozen in liquid N2, stored in single-use

128   aliquots at -80 °C and thawed by incubating at 37 °C Supplementary Figure 3). We found that

129   freeze-thaw increased CR3022 binding to the 2P spike relative to the fresh sample, although

130   incubation at 37 °C of the thawed sample for 20 min reduced binding close to the levels

131   observed in the fresh sample. Based on these data, in order to obtain consistent results in

132   binding studies, we recommend flash-freezing spike samples in single use aliquots, thawing at

133   37 °C followed by a brief (~20 min) incubation at 37 °C before using the 2P spike in binding

134   studies.

135   These results suggested that cold-induced denaturation of spike was associated with

136   increased RBD-exposure of the S ectodomain, and we thus asked whether a "down" state

137   stabilized S ectodomain might be resistant to cold-induced denaturation (Figure 2). We included

138   in this analysis a variant that combined the recently described rS2d[9] and HexaPro mutations[11]

139   (Figure 2a,b). This new variant, named rS2d-HexaPro, showed the highest production yields of

140   the all-RBD-down spike constructs (Figure 2c). Similar to the rS2d construct[9], rS2d-Hexapro

141   was shown by NSEM to be 100 % in a 3-RBD-down conformation (Figure 2d,e, Extended Data

142   Figure 7 and Supplementary Movie 1). Both HexaPro and rS2d-HexaPro appeared more

143   resistant to cold-induced denaturation (Figure 2f) than the 2P spike (Figure 1e), with rS2d-

144   HexaPro showing a higher intact spike percentage than HexaPro (Figure 2f). The rS2d

145   mutations (D985C, S383C) introduce an inter-protomer disulfide bond between the RBD and the

146   S2 domain, which we suggest stabilizes the spike and prevents its cold-induced denaturation.

147   An independent study also reported that the 985C-383C disulfide bond, as well as an introduced

148   disulfide between residues 987 and 413, prevented denaturation of the spike when stored at 4

149   °C[15]. These data suggest that inter-promoter disulfide linkages may be a general strategy for

150   stabilization of the 2P spike ectodomain and preventing its cold-induced denaturation.   We also

151   included two glycan-deleted mutants, 2P-N165A and 2P-N234A[16], that favor the RBD "up" or

152   "down" conformation, respectively (Figure 2f), and both mutants showed substantial reduction of

153   spike percentage after incubation at 4 °C (Figure 2f), Thermostability and binding studies

154   (Figures 2g,h) further confirmed that both HexaPro and rS2d-HexaPro were more resistant to

155   cold destabilization compared to the 2P version (Figure 1). ACE-2 binding to rS2d-HexaPro was

156   substantially reduced for samples stored at all temperatures, as expected for a spike construct

157   fixed in an RBD-down conformation. Similarly, binding to 2G12 remained same for the rS2d-

158   HexaPro construct irrespective of the storage temperature of the 2P spike (Figure 1h), showing

159   that the rS2d-Hexapro structure remains unperturbed upon 4 °C storage. For HexaPro, binding

160   to ACE-2 was higher and 2G12 binding was reduced with 4 °C -stored protein compared to 37

161   °C-stored samples, showing that the HexaPro structure remained susceptible to perturbation at

162   lower temperatures.

163   Overall, our results demonstrate the cold sensitivity of the furin-cleavage deficient

164   SARS-CoV-2 ectodomain, and its impact on antibody and receptor binding. We have also

165   shown that this cold destabilization is substantially reduced in the HexaPro spike and further

166   reduced by stabilization of the S ectodomain in a disulfide-locked "down" position.

167   **Acknowledgements**

180   **Author contributions**

181   R.J.E., K.Mansouri., V.S. and P.A. discovered the effect of storage temperature on spike

182   stability. R.J.E. led NSEM studies and established quantitative metrics for spike QC. K.Mansouri

183   collected NSEM data and performed analyses. V.S. purified proteins and performed

184   thermostability measurements. K.Manne purified proteins, performed SPR assays, prepared

185   samples for NSEM, Tycho, ELISA, SPR and DSC measurements, and coordinated the study

186   between the different research teams. B.W. performed DSC measurements. R.P., M.D. J.S. and

187   W.W. performed ELISA assays. D.L., X.L., K.S. and G.S. isolated antibodies from convalescent

188   patient. S.G. and K. J. purified proteins and performed thermostability assays. M.F.K purified

189   proteins. Z.M. performed binding measurements. R.H. initiated the DSC experiments and

190   provided the rS2d, 2P-N234A and 2P-N165A constructs prior to publication. M.A. supervised

191   the DSC experiments. B.F.H. supervised ELISA experiments and antibody isolation. P.A.

192   oversaw and led the study, and co-wrote the paper with R.J.E. and V.S. All authors reviewed

193   and commented on the manuscript.

194

195 **Methods**

196 *Protein expression and purification*

197   SARS-CoV-2 ectodomain constructs were produced and purified [1,11] as follows. A gene

198 encoding residues 1−1208 of the SARS-CoV-2 S (GenBank: MN908947) with proline

199 substitutions at residues 986 and 987, a "GSAS" substitution at the furin cleavage site (residues

200 682–685), a C-terminal T4 fibritin trimerization motif, an HRV3C protease cleavage site, a

201 TwinStrepTag and an 8XHisTag was synthesized and cloned into the mammalian expression

202 vector pαH. Plasmids were transiently transfected into either FreeStyle-293F cells using

203 Turbo293 (SpeedBiosystems). Cells were grown in a 37 °C incubator with 9 % CO2 and 120

204 rpm rotary motion. Protein was purified on the sixth day post-transfection from filtered

205 supernatant using StrepTactin resin (IBA), followed by SEC purification using a Superose 6

206 10/300 Increase column in nCoV buffer (2mM Tris, pH 8.0, 200 mM NaCl, 0.02% sodium azide).

207 rS2d-Hexapro was also grown in CHO cells. Plasmids were transiently transfected into CHO

208 cells using ExpiFectamine CHO Transfection Kit (ThermoFisher), and protein was purified one

209 the sixth day post-transfection. All protein purification steps including Strep tag purification and

210 SEC were performed at room temperature. The spikes were purified the same day that the cells

211 are harvested and the purification is completed 6-8 hours. The purified protein is flash frozen

212 and stored in -80 °C in single-use aliquots. Each aliquot is thawed and briefly incubated (~20

213 min) at 37 °C before use.

214   Antibodies were produced in Expi293 cells and purified by Protein A affinity. For ACE-2

215 constructs, the ACE-2 C-terminus was fused with either the human or mouse Fc region

216 including C-terminal 6X His-tag on the Fc domain. ACE-2 with human Fc tag was purified by

217 Protein A affinity chromatography, and ACE-2 with mouse F_C tag was purified by Ni-NTA

218 chromatography.

219

220 *Negative-stain electron microscopy*

221 Spike samples were pre-incubated (stored) for specified times in nCoV buffer at 4, 22 or 37 °C,

222 then moved to room temperature for preparation of NSEM grids, which was complete in less

223 than 5 min. Samples were diluted to 100 µg/ml with room-temperature buffer containing 20 mM

224 HEPES pH 7.4, 150 mM NaCl, 5% glycerol and 7.5 mM glutaraldehyde, and incubated 5 min;

225 then glutaraldehyde was quenched for 5 min by addition of 1M Tris stock to a final concentration

226 of 75 mM. A 5-µl drop of sample was applied to a glow-discharged, carbon-coated grid for 10-15

227 s, blotted, stained with 2% uranyl formate, blotted and air-dried. Images were obtained with a

228 Philips EM420 electron microscope at 120 kV, 82,000× magnification, and a 4.02 Å pixel size.

229 The RELION program [17] was used for particle picking, 2D and 3D class averaging.

230 *Thermostability assays*

231 Thermostability of the S ectodomain samples were measured using DSF and DSC.

232 Samples were purified and buffer exchanged into HBS buffer (10 mM HEPES, 150 mM NaCl,

233 pH 7.4) by SEC on a Superose 6 10/300 column. DSF assay was performed using Tycho NT. 6

234 (NanoTemper Technologies). Spike variants were diluted (0.15 mg/ml) in HBS and run in

235 triplicate. Intrinsic fluorescence was recorded at 330 nm and 350 nm while heating the sample

236 from 35–95 °C at a rate of 30 °C/min. The ratio of fluorescence (350/330 nm) and inflection

237 temperatures (T_i) were calculated by Tycho NT. 6.

238 DSC measurements were performed using the NanoDSC platform (TA instruments; New

239 Castle, DE). Samples that had been incubated at 22 ºC or 37 ºC were purified by SEC at room

240 temperature and the sample incubated at 4 ºC was purified by SEC at 4 ºC (Extended Data Figure

241 2), diluted to 0.2–0.3 mg/mL in HBS, and degassed for 15 min at room temperature prior to

242 analysis. DSC measurements were performed immediately after SEC purification of the

243   samples. DSC cells were conditioned with filtered, degassed HBS prior to sample loading.

244   Protein samples were heated from 10 °C to 100 °C at 1 °C/min under 3 atm pressure using HBS

245   as the reference buffer. The observed denaturation profiles were buffer subtracted, converted to

246   molar heat capacity, baseline-corrected with a 6th-order polynomial, and fit with 2-4 Gaussian

247   transition models, as needed, using the NanoAnalyze software (TA Instruments). The peak

248   transition temperature (T_m) is reported as the temperature at the maximum observed heat

249   capacity of each transition peak.

250   *Isolation of antibodies from COVID-19 convalescent donors*

251   Human SARS-CoV-2 Spike antibodies Ab712199 and Ab511584 were isolated from a COVID-

252   19 convalescent individual. Peripheral blood was collected following informed consent on a

253   Duke University Medical Center approved Institutional Review Board protocol. Briefly, PBMC

254   samples collected after the onset of the symptoms were stained and the memory B cells were

255   sorted with SARS-CoV-2 Spike-2p probes. Antibody IgH and IgK/L genes were recovered from

256   the single-cell sorted cells, cloned into human IgG1 constant region backbone, and purified by

257   Protein A beads as previously described [18].

258   *ELISA assays*

259   Spike samples were pre-incubated at different temperatures then tested for antibody- or ACE-2-

260   binding in ELISA assays as previously described [19,20]. Assays were run in two formats. In the

261   first format antibodies or ACE-2 protein were coated on 384-well plates at 2 µg/ml overnight at

262   4°C, washed, blocked and followed by two-fold serially diluted spike protein starting at 25 µg/ml.

263   Binding was detected with polyclonal anti-SARS-CoV-2 spike rabbit serum (developed in our

264   lab), followed by goat anti-rabbit-HRP (Abcam #ab97080) and TMB substrate (Sera Care Life

265   Sciences #5120-0083). Absorbance was read at 450 nm. In the second format, serially diluted

266   spike protein was bound in individual wells of 384-well plates, which were previously coated with

267   streptavidin (Thermo Fisher Scientific #S-888) at 2 µg/ml and blocked. Proteins were incubated

268   at room temperature for 1 hour, washed, then human mAbs were added at 10 µg/ml. Antibodies

269   were incubated at room temperature for 1 hour, washed and binding detected with goat anti-

270   human-HRP (Jackson ImmunoResearch Laboratories, #109-035-098) and TMB substrate.

271   Commercially obtained constructs of SARS-CoV-2 spike ectodomain (S1+S2 ECD, S2

272   ECD and RBD) (Sino Biological Inc cat# 40589-V08B1 and 40590-V08B respectively and RBD

273   from Genescript cat# Z03483) were coated directly on 384-well plates at 2 µg/ml and incubated

274   overnight at 4 °C. Plates were washed, blocked and human mAbs three-fold serially diluted from

275   100 µg/ml were added for 1 hour at room temp followed by washing. Binding was detected with

276   Goat anti-human IgG-HRP followed by TMB substrate.

277

278   *Microneutralization assay*

279   Live SARS-CoV-2 Microneutralization (MN) assays were adapted from Berry et al.[21] In short,

280   sera or purified antibodies are diluted two-fold and incubated with 100 TCID50 virus for 1 hour.

281   These dilutions are used as the input material for a TCID50. Each batch of MN includes known

282   neutralizing and non-neutralizing controls. Data are reported as the last concentration at which a

283   test sample protects Vero E6 cells. Recently, a fluorescent infectious clone of SARS-CoV-2 was

284   developed[22].

285   *Plaque Reduction Neutralization Test (PRNT)*

286   Live SARS-CoV-2 Plaque Reduction Neutralization Test (PRNT) was performed in an assay

287   adapted from Berry et al.[21] Briefly, two-fold dilutions of a test sample (serum, plasma, purified

288   Ab) are incubated with 50 PFU SARS-CoV-2 for 1 hour (NR-52281; BEI Resources). The

289   antibody/virus mixture was then used to inoculate Vero E6 cells (ATCC). Cultures were then

290   incubated at 37°C, 5% CO_2 for one hour. At the end of the incubation, 1 mL of a viscous overlay

291   (1:1 2X DMEM and 1.2% methylcellulose) was added to each well. Plates were incubated for 4

292   days. After fixation, staining and washing, plates were dried and plaques counted. Known

293 neutralizing and non-neutralizing antibodies/sera are included in this assay as positive and

294 negative controls, respectively. Plaques from each dilution of each sample are counted and

295 data are reported as the concentration at which 50% of input virus is neutralized.

296

297 *Pseudovirus Neutralization Assay*

298 SARS-CoV-2 neutralization was assessed with Spike-pseudotyped viruses in 293T/ACE2 cells

299 as a function of reductions in luciferase (Luc) reporter activity. 293T/ACE2 cells were kindly

300 provided by Drs. Mike Farzan and Huihui Mu at Scripps. Cells were maintained in DMEM

301 containing 10% FBS and 3 µg/ml puromycin. An expression plasmid encoding codon-optimized

302 full-length Spike of the Wuhan-1 strain (VRC7480), was provided by Drs. Barney Graham and

303 Kizzmekia Corbett at the Vaccine Research Center, National Institutes of Health (USA). The

304 D614G amino acid change was introduced into VRC7480 by site-directed mutagenesis using

305 the QuikChange Lightning Site-Directed Mutagenesis Kit from Agilent Technologies (Catalog #

306 210518). The mutation was confirmed by full-length Spike gene sequencing. Pseudovirions

307 were produced in HEK 293T/17 cells (ATCC cat. no. CRL-11268) by transfection using Fugene

308 6 (Promega Cat#E2692) and a combination of Spike plasmid, lentiviral backbone plasmid

309 (pCMV ΔR8.2) and firefly Luc reporter gene plasmid (pHR' CMV Luc)[23] in a 1:17:17 ratio.

310 Transfections were allowed to proceed for 16-20 hours at 37°C. Medium was removed,

311 monolayers rinsed with growth medium, and 15 ml of fresh growth medium added. Pseudovirus-

312 containing culture medium was collected after an additional 2 days of incubation and was

313 clarified of cells by low-speed centrifugation and 0.45 µm micron filtration and stored in aliquots

314 at -80°C. TCID$_{50}$ assays were performed on thawed aliquots to determine the infectious dose for

315 neutralization assays (RLU 500-1000x background, background usually averages 50-100 RLU).

316

317 For neutralization, a pre-titrated dose of virus was incubated with 8 serial 3-fold or 5-fold

318 dilutions of serum samples or mAbs in duplicate in a total volume of 150 µl for 1 hr at 37°C in

319   96-well flat-bottom poly-L-lysine-coated culture plates (Corning Biocoat). Cells were suspended

320   using TrypLE express enzyme solution (Thermo Fisher Scientific) and immediately added to all

321   wells (10,000 cells in 100 µL of growth medium per well). One set of 8 control wells received

322   cells + virus (virus control) and another set of 8 wells received cells only (background control).

323   After 66-72 hrs of incubation, medium was removed by gentle aspiration and 30 µL of Promega

324   1X lysis buffer was added to all wells. After a 10 minute incubation at room temperature, 100 µL

325   of Bright-Glo luciferase reagent was added to all wells. After 1-2 minutes, 110 µL of the cell

326   lysate was transferred to a black/white plate (Perkin-Elmer). Luminescence was measured

327   using a PerkinElmer Life Sciences, Model Victor2 luminometer. Neutralization titers are the

328   serum dilution (ID50/ID80) or mAb concentration (IC50/IC80) at which relative luminescence

329   units (RLU) were reduced by 50% and 80% compared to virus control wells after subtraction of

330   background RLUs. Maximum percent inhibition (MPI) is the % neutralization at the lowest serum

331   dilution or highest mAb concentration tested. Serum samples were heat-inactivated for 30

332   minutes at 56 °C prior to assay.

333   *Surface Plasmon Resonance*

334   Antibody binding to SARS-CoV-2 spike constructs was assessed by surface plasmon

335   resonance on a Biacore T-200 (GE-Healthcare) with HBS buffer with 3 mM EDTA and 0.05%

336   surfactant P-20 added. For the data presented in Figure 1H and Supplementary Figure 2, spike

337   samples that were incubated at 4 °C, 22 °C and 37 °C for a week, were held in the sample

338   chamber at 8 °C, 22 °C and 37 °C, respectively, during the SPR run. For the SPR data

339   presented in Extended Data Figures 4 and 7, the sample incubated at 4 °C for a week was held

340   in the sample chamber at 8 °C, and the samples incubated at 22 °C and 37 °C for a week, were

341   held in the sample chamber at 22 °C during the run. The flow cell was maintained at 25 °C, thus

342   all binding assays were performed at 25 °C. Antibodies captured on a CM5 chip coated with

343   amine-coupled human Anti-Fc (8000RU) were assayed by SARS-CoV-2 spike at 200 nM. The

344   surface was regenerated between injections with 3 M $MgCl_2$ solution for 10 s at 100 µl/min.

345   Sensorgram data were analyzed using the BiaEvaluation software (GE Healthcare).

346

347   *Cryo-EM*

348   Purified SARS-CoV-2 spike preparations were diluted to a concentration of ~1 mg/mL in 2 mM

349   Tris pH 8.0, 200 mM NaCl and 0.02% NaN_3. A 2.5-µL drop of protein was deposited on a CF-

350   1.2/1.3 grid that had been glow discharged for 30 seconds in a PELCO easiGlow™ Glow

351   Discharge Cleaning System. After a 30 s incubation in >95% humidity, excess protein was

352   blotted away for 2.5 seconds before being plunge frozen into liquid ethane using a Leica EM

353   GP2 plunge freezer (Leica Microsystems). Frozen grids were imaged in a Titan Krios (Thermo

354   Fisher) equipped with a K3 detector (Gatan).

355   **Data Availability**

356   The datasets generated the current study are available from the corresponding author on
357   reasonable request.

References

358 **References**

359 1   Wrapp, D. *et al.* Cryo-EM structure of the 2019-nCoV spike in the prefusion
360   conformation. *Science* **367**, 1260-1263, doi:10.1126/science.abb2507 (2020).
361 2   Walls, A. C. *et al.* Structure, Function, and Antigenicity of the SARS-CoV-2 Spike
362   Glycoprotein. *Cell* **181**, 281-292 e286, doi:10.1016/j.cell.2020.02.058 (2020).
363 3   Barnes, C. O. *et al.* Structures of human antibodies bound to SARS-CoV-2 spike reveal
364   common epitopes and recurrent features of antibodies. *bioRxiv*,
365   doi:10.1101/2020.05.28.121533 (2020).
366 4   Pinto, D. *et al.* Cross-neutralization of SARS-CoV-2 by a human monoclonal SARS-CoV
367   antibody. *Nature*, doi:10.1038/s41586-020-2349-y (2020).
368 5   Mire, C. E. *et al.* A Cross-Reactive Humanized Monoclonal Antibody Targeting Fusion
369   Glycoprotein Function Protects Ferrets Against Lethal Nipah Virus and Hendra Virus
370   Infection. *J Infect Dis* **221**, S471-S479, doi:10.1093/infdis/jiz515 (2020).
371 6   Ke, Z., Oton, J.; Qu, K.; Cortese, M.; Zila, V.; McKeane, L.; Nakane, T.; Zivanov, J.;
372   Neufeldt, C.J.; Lu, J.M.; Peukes, J.; Xiong, X.; Krausslich, H.G.; Scheres, S.H.W.;
373   Bartenschlager, R.; Briggs, J.A.G. Structures, conformations and distributions of SARS-
374   CoV-2 spike protein trimers on intact virions. *bioRxiv* (2020).
375 7   Liu, L. *et al.* Potent Neutralizing Monoclonal Antibodies Directed to Multiple Epitopes on
376   the SARS-CoV-2 Spike. *bioRxiv*, doi:10.1101/2020.06.17.153486 (2020).
377 8   Zhou, T. *et al.* Structure-Based Design with Tag-Based Purification and In-Process
378   Biotinylation Enable Streamlined Development of SARS-CoV-2 Spike Molecular Probes.
379   *bioRxiv*, doi:10.1101/2020.06.22.166033 (2020).
380 9   Henderson, R. *et al.* Controlling the SARS-CoV-2 spike glycoprotein conformation. *Nat
381   Struct Mol Biol*, doi:10.1038/s41594-020-0479-4 (2020).
382 10   Magnusson, A. O. *et al.* nanoDSF as screening tool for enzyme libraries and
383   biotechnology development. *FEBS J* **286**, 184-204, doi:10.1111/febs.14696 (2019).
384 11   Hsieh, C. L. *et al.* Structure-based design of prefusion-stabilized SARS-CoV-2 spikes.
385   *Science*, doi:10.1126/science.abd0826 (2020).
386 12   Zhou, T. *et al.* A pH-dependent switch mediates conformational masking of SARS-CoV-2
387   spike. *bioRxiv*, doi:10.1101/2020.07.04.187989 (2020).
388 13   Good, N. E. *et al.* Hydrogen ion buffers for biological research. *Biochemistry* **5**, 467-477,
389   doi:10.1021/bi00866a011 (1966).
390 14   Acharya, P. *et al.* A glycan cluster on the SARS-CoV-2 spike ectodomain is recognized
391   by Fab-dimerized glycan-reactive antibodies. *bioRxiv*, doi:10.1101/2020.06.30.178897
392   (2020).
393 15   Xiong, X. *et al.* A thermostable, closed SARS-CoV-2 spike protein trimer. *Nat Struct Mol
394   Biol*, doi:10.1038/s41594-020-0478-5 (2020).
395 16   Henderson, R. *et al.* Glycans on the SARS-CoV-2 Spike Control the Receptor Binding
396   Domain Conformation. *bioRxiv*, doi:10.1101/2020.06.26.173765 (2020).
397 17   Scheres, S. H. W. in *Methods in Enzymology* Vol. 579 (ed R. A. Crowther) 125-157
398   (Academic Press, 2016).
399 18   Liao, H. X. *et al.* Co-evolution of a broadly neutralizing HIV-1 antibody and founder virus.
400   *Nature* **496**, 469-476, doi:10.1038/nature12053 (2013).
401 19   Alam, S. M. *et al.* Mimicry of an HIV broadly neutralizing antibody epitope with a
402   synthetic glycopeptide. *Science translational medicine* **9**,
403   doi:10.1126/scitranslmed.aai7521 (2017).
404 20   Bonsignori, M. *et al.* Staged induction of HIV-1 glycan-dependent broadly neutralizing
405   antibodies. *Science translational medicine* **9**, doi:10.1126/scitranslmed.aai7514 (2017).

406   21   Berry, J. D. *et al.* Development and characterisation of neutralising monoclonal antibody
407   to the SARS-coronavirus. *J Virol Methods* **120**, 87-96,
408   doi:10.1016/j.jviromet.2004.04.009 (2004).
409   22   Xie, X. *et al.* An Infectious cDNA Clone of SARS-CoV-2. *Cell Host Microbe* **27**, 841-848
410   e843, doi:10.1016/j.chom.2020.04.004 (2020).
411   23   Naldini, L. *et al.* In vivo gene delivery and stable transduction of nondividing cells by a
412   lentiviral vector. *Science* **272**, 263-267, doi:10.1126/science.272.5259.263 (1996).

413

414

a

SARS-CoV-2 S

| S1 | | | | | | | S2 | | | | | |

NTD — RBD — SD2 — S2' — HR1 — CD — TM — CT

SD1
S1/S2
Cleavage site
FP
CH
HR2
1208
1273

Stabilized S
ectodomain (2P)

NTD — RBD — SD2 — S2' — HR1 — 2 Pro — CD — Foldon — TwinStrep — 8XHis

SD1
GSAS
FP
CH
HR2
HRV3C

b
Fresh

c
4 ℃, 7 d

d
4 ℃ , 7d → 37℃, 3 h

100 nm

e

f

g

h

CR3022 binding

2G12 binding

37 ℃, 7 d
22 ℃, 7 d
4 ℃, 7 d
4 ℃ , 7d → 37℃
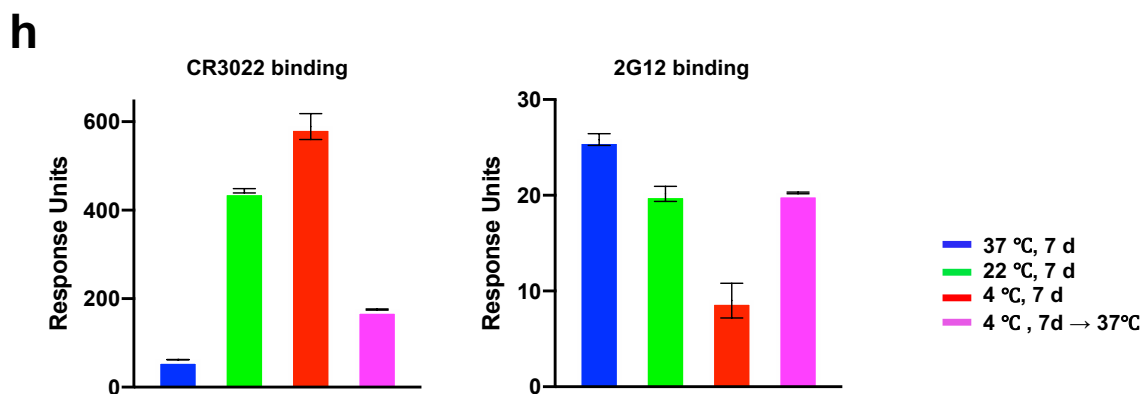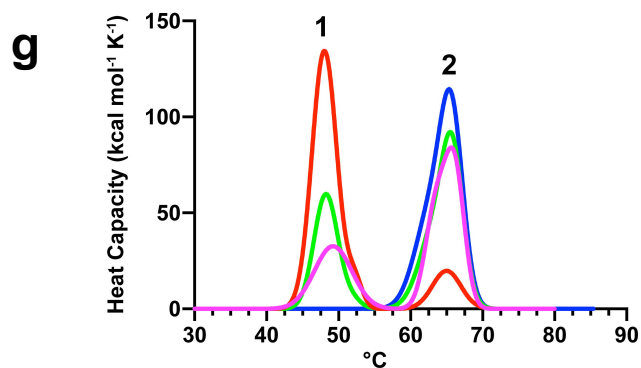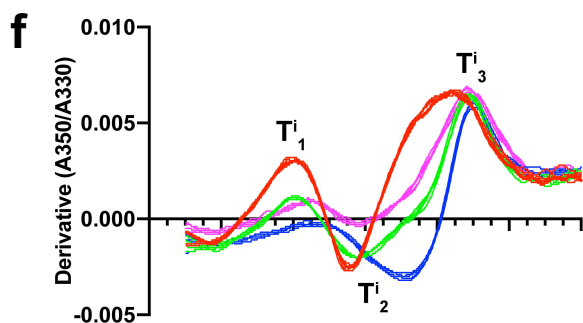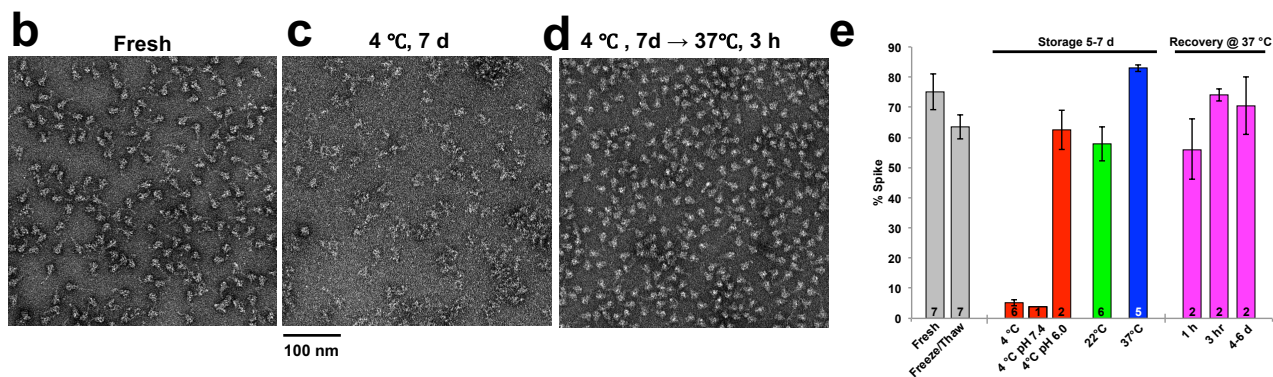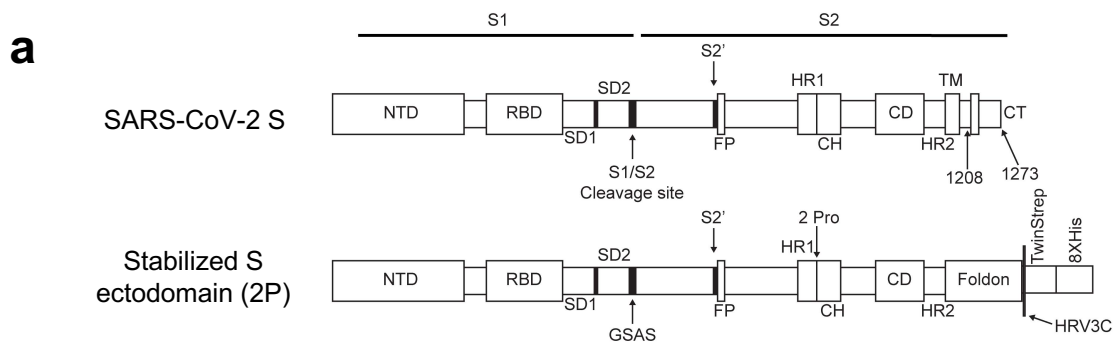
Figure 1. Temperature-dependence of the SARS-CoV-2 S ectodomain. (a) Schematic of the SARS-CoV-2 spike (top) and a furin cleavage-deficient, soluble, stabilized ectodomain construct (bottom). **(b-d)** Representative NSEM micrograph from **(b)** a freshly prepared sample of the S ectodomain, **(c)** the same sample after storing the protein for one week at 4 °C, **(d)** the same sample after storing the protein for one week at 4 °C followed by a 3-hour incubation at 37 °C. **(e)** Bar graph summarizing NSEM results on S ectodomain samples stored under different conditions. From left to right, bars show spike percentage in a fresh sample of spike; after the spike undergoes a single freeze-thaw cycle; after it has been incubated for 5-7 days at 4 °C (red), 22 °C (green) or 37 °C (blue); and spike samples that were stored for 1 week at 4 °C, then incubated at 37 °C for 1 hour, 3 hours, or 4-6 days. Solid bars indicate averages, with number of samples indicated at the bottom of each column. The error bars indicate standard error of the mean, except when N=2, where the error bars indicate range. **(f)** DSF profiles obtained by following changes in intrinsic fluorescence upon applying a thermal ramp to the sample and expressed as the first derivative of the ratio between fluorescence at 350 nm and 330 nm. Maxima and minima indicate inflection temperatures, T^i. For each data point, 5 overlaid curves are shown indicating technical replicates. **(g)** DSC profiles, shown as representative of two technical repeats. **(h)** Antibody CR3022 IgG (left) and 2G12 IgG (right) binding to spike stored at different temperatures measured by SPR. Data for spike samples measured after a 1-week incubation at 37, 22, and 4 °C, are shown in blue, green, and red respectively; sample stored 1 week at 4 °C and then incubated for 6 hours at 37 °C shown in magenta. During the SPR run the sample chamber was maintained at temperatures of 37 °C, 22 °C and 8 °C, for the 37 °C, 22 °C and 4 °C incubated samples, respectively. The binding experiments were carried out at 25 °C. Error bars are derived from 3 technical repeats. The data shown are representative of at least 5 independent experiments. 2 independent repeats using separate protein lots are shown in Supplementary Figure 2.

a HexaPro (PDB ID: 6XKL)

b rS2d (PDB ID: 6X29)

c

d rS2d-HexaPro

100 nm

10 nm

e rS2d-HexaPro

50 Å

f

g HexaPro   rS2d-HexaPro

— 37 ℃, 7 d
— 22 ℃, 7 d
— 4 ℃, 7 d
— 4 ℃ , 7d → 37℃

h HexaPro

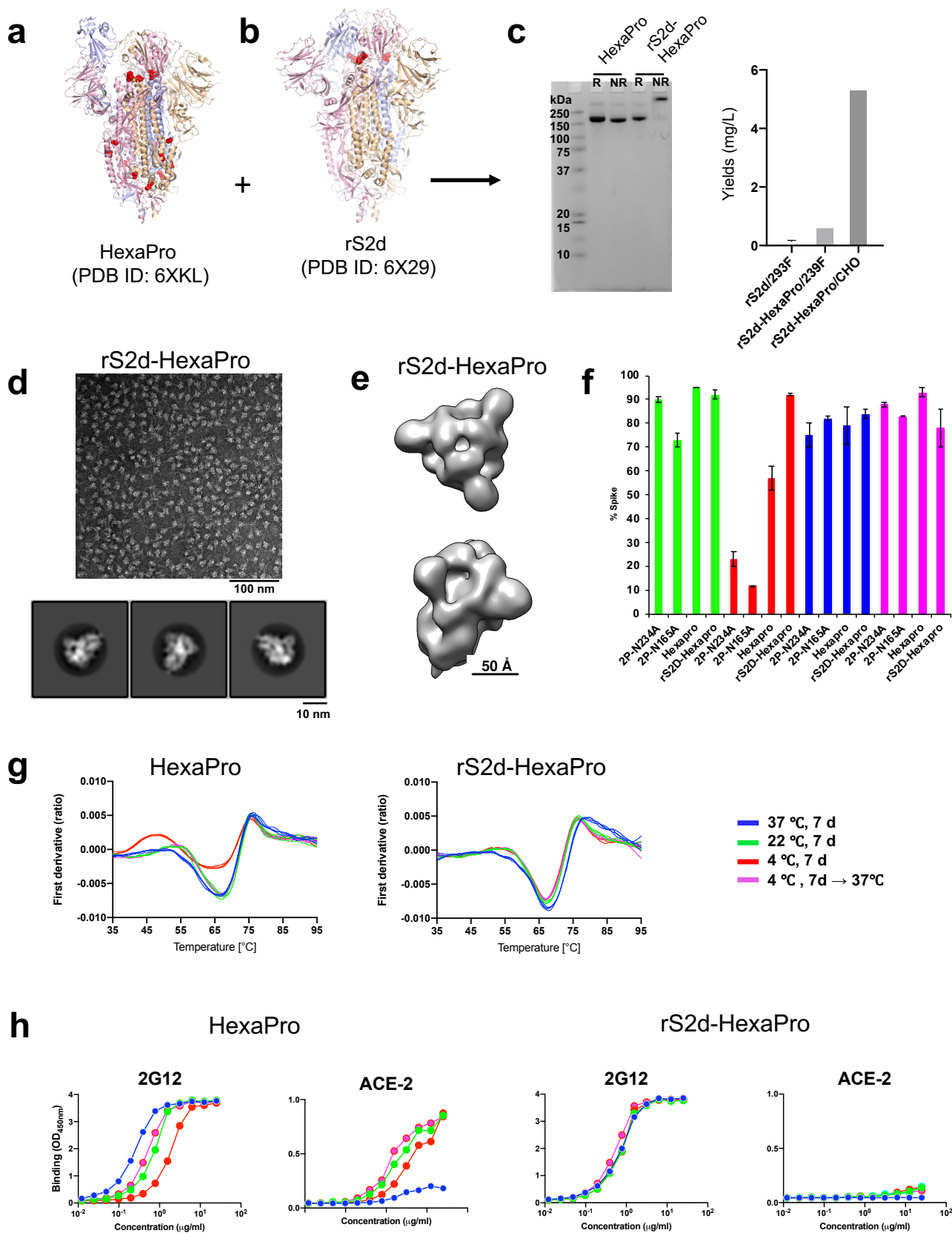2G12   ACE-2

rS2d-HexaPro

2G12   ACE-2

Figure 2. Engineered SARS-CoV-2 spike variant, rS2d-HexaPro, is resistant to temperature-dependent structural changes. (a-b) Structures of **(a)** HexaPro showing a 1-RBD-up conformation (PDB ID: 6X29) and **(b)** rS2d (PDB ID: 6XKL) showing a all-RBD-down conformation. **(c)** *(left)* SDS-PAGE. Lane 1: Molecular weight marker, Lanes 2 and 3: HexaPro, Lane 4 and 5: rS2d-HexaPro. R= Reducing, and NR = Non-reducing conditions. *(right)* Bar graph summarizing protein yields in mg/L of culture for, from left to right, rS2d produced in 293F cells, rS2d-HexaPro produced in Freestyle 293F cells, and rS2d-HexaPro expressed in CHO cells. **(d)** *(top)* Representative NSEM micrograph from a preparation of rS2d-Hexapro and *(bottom)* 2D class averages. **(e)** 3D reconstruction of rS2d-Hexapro obtained from NSEM data. **(f)** Bar graph summarizing results from NSEM on spike variants stored at different temperatures. Error bars shown are derived from at least two independent experiments with dfferent protein lots, and represent standard error of mean where N ≥ 3 and range where N=2. **(g)** DSF profiles for Hexapro (left) and rS2d-Hexapro (right). **(h)** Binding of 2G12 and ACE-2 to Hexapro (left) and rS2d-Hexapro (right) measured by ELISA. Serially diluted spike protein was bound in individual wells of 384-well plates, which were previously coated with streptavidin. Proteins were incubated and washed, then 2G12 at 10 µg/ml or ACE-2 with a mouse Fc tag at 2 µg/ml were added. Antibodies were incubated, washed and binding detected with goat anti-human-HRP.
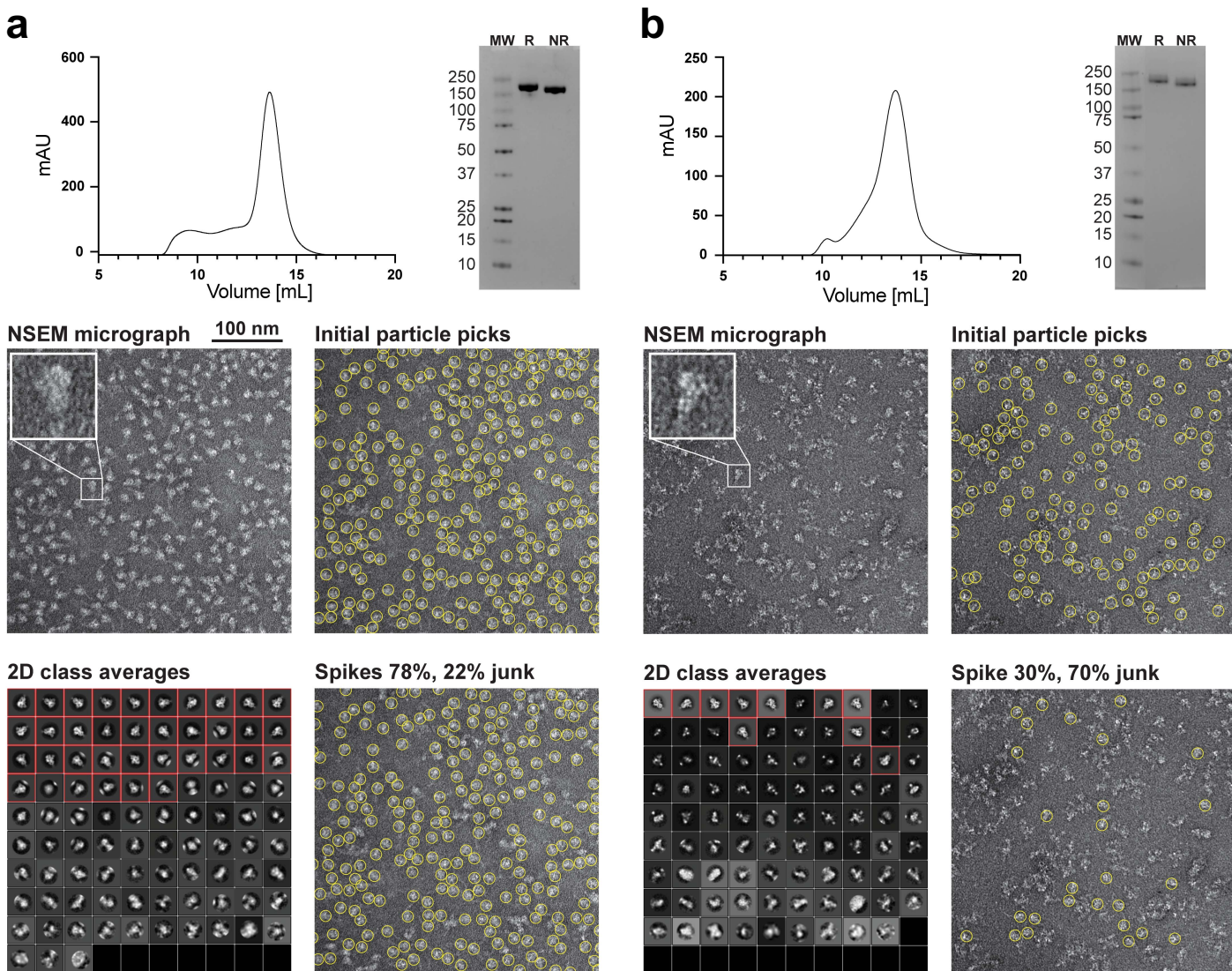
Extended Data Figure 1. Purification and quality control of the SARS-CoV-2 S protein ectodomain. (a and b) Two representative spike preparations that together highlight the role of NSEM in discriminating between good **(a)** and bad **(b)** spike preparations that otherwise appear to be of similar quality by SEC (top, left) and SDS-PAGE (top, right). Representative micrographs from each prep are shown, middle left. Protein appears as white blobs on gray background. Insets show a single kite-shaped spike particle enlarged. At the middle right, automatic particle picking is shown as yellow circles superimposed on the micrograph. Sets of ~20,000 initial particles picks are subjected to automated 2D classification to group together and average particles with similar features into discrete classes, bottom left. In the 2D class averages for each sample, the classes that contain the SARS-Cov-2 S ectodomain (shown within red boxes) can be clearly distinguished from classes that contain junk. The final spike picks come from the particles contained within the indicated classes and their total number provide an estimate of the ratio between the SARS-CoV-2 S ectodomain and junk seen in the NSEM sample.
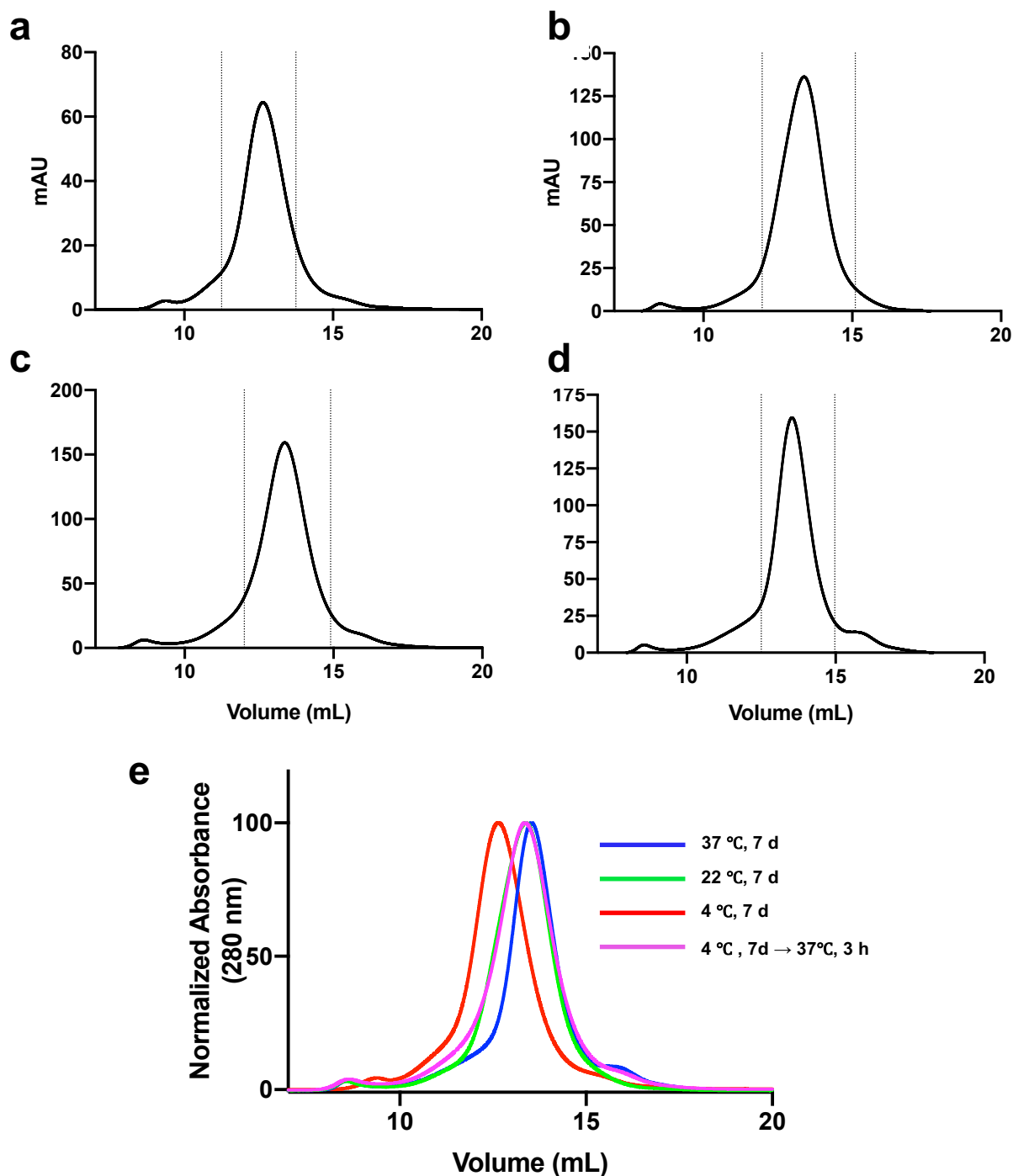
Extended Data Figure 2. Size Exclusion Chromatography of SARS-CoV-2 S ectodomain incubated at different temperatures. SEC profiles run on a Superose 6 increase 10/300 column for SARS-CoV-2 S ectodomain samples that were incubated at **(a)** 4 °C for one week, **(b)** 22 °C for one week. **(c)** 37 °C for one week, and **(d)** 4 °C for one week and moved to 37 °C for 3 hours prior to the experiment. **(e)** Overlay of SEC plots normalized to allow better visualization of peak shifts.
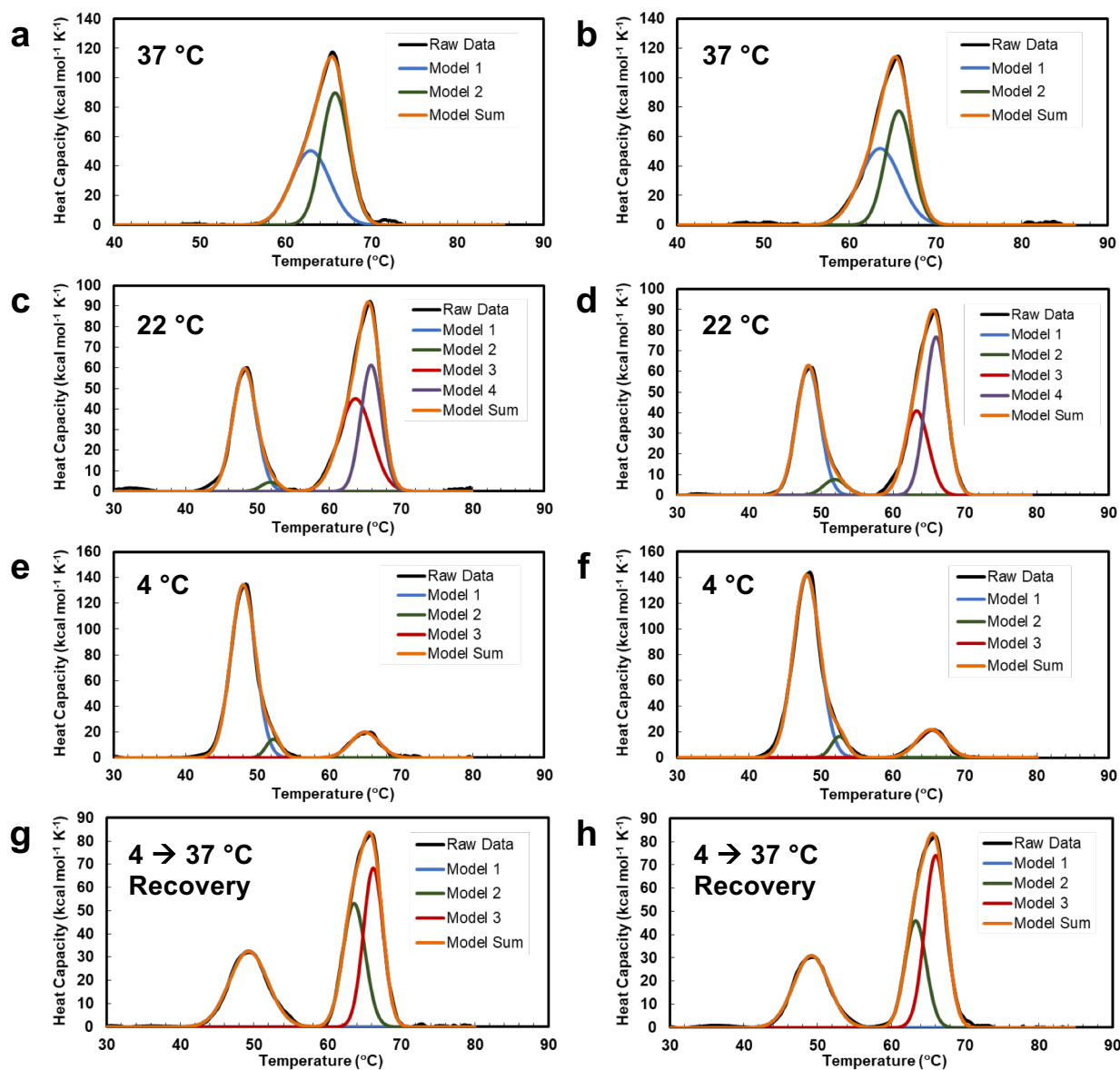
	Transition Peak 1		Transition Peak 2		DSC Model Fits			
	T_{onset} (°C)	T_m (°C)	T_{onset} (°C)	T_m (°C)	$T_{m,1}$ (°C)	$T_{m,2}$ (°C)	$T_{m,3}$ (°C)	$T_{m,4}$ (°C)
37 °C	N/A	**N/A**	57.5 ± 0.4	**65.5 ± 0.2**	63.2 ± 0.7	65.74 ± 0.02	N/A	N/A
22 °C	43.64 ± 0.02	**48.2 ± 0.1**	59 ± 1	**65.8 ± 0.1**	48.2 ± 0.1	51.87 ± 0.03	63.5 ± 0.5	65.9 ± 0.1
4 °C	43.0 ± 0.4	**48.41 ± 0.01**	61.1 ± 0.2	**65.1 ± 0.3**	48.02 ± 0.03	52.4 ± 0.3	65.1 ± 0.3	N/A
4 → 37 °C Recovery	42.5 ± 0.5	**49.2 ± 0.1**	59.59 ± 0.04	**65.95 ± 0.02**	49.2 ± 0.1	63.4 ± 0.3	66.1 ± 0.2	N/A

Extended Data Figure 3. Thermostability of the SARS-CoV-2 spike ectodomain stored at different temperatures. Representative thermal denaturation profiles of the SARS-CoV-2 spike ectodomain after 1 week incubations at (**a,b**) 37 °C , (**c,d**) 22 °C, (**e,f**) 4 °C, and (**g,h**) 4 °C followed by 37 °C for 3 hours. Profiles and transition parameters (**I**) were obtained by DSC and analyzed as described in Methods. Raw data (black) was best fit with two or more Gaussian transition models ($T_{m,1-4}$) (blue, green, red, purple). The peak observed at ~65 °C was best fit with two Gaussian transition models suggesting a complex unfolding mechanism. Data shown are the mean and range from two experimental replicates.
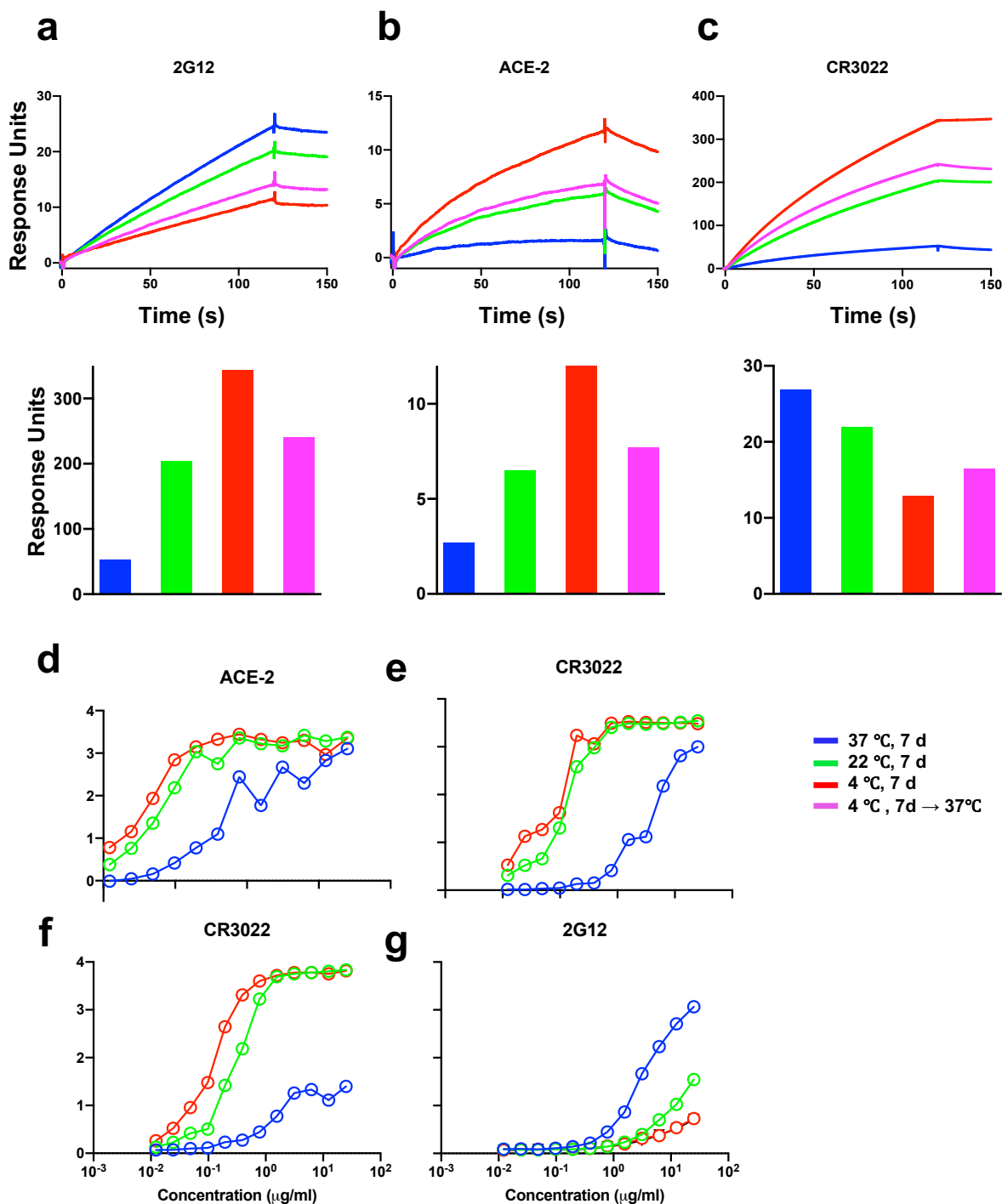
Extended Data Figure 4. Changes in antigenicity of SARS-CoV-2 S ectodomain incubated at different temperatures. (a-c) SPR profiles showing binding of **(a)** ACE-2, **(b)** RBD-directed antibody, CR3022, and **(c)** S2 glycan-directed antibody 2G12 to spike samples incubated for 1 week at either 37 °C (blue), 22 °C (green) or 4 °C (red). Binding to spike sample first incubated at 4 °C for 1 week, then moved to 37 °C for 3 hours prior to the experiment is shown in magenta. **(d-g)** ELISA binding profiles showing binding of **(d)** ACE-2, **(e)** RBD-directed antibody, CR3022, in a format where antibody was coated on the plate (see methods) and **(f)** CR3022 and **(g)** 2G12, in a format where spike was captured on a strep-coated plate (see methods).
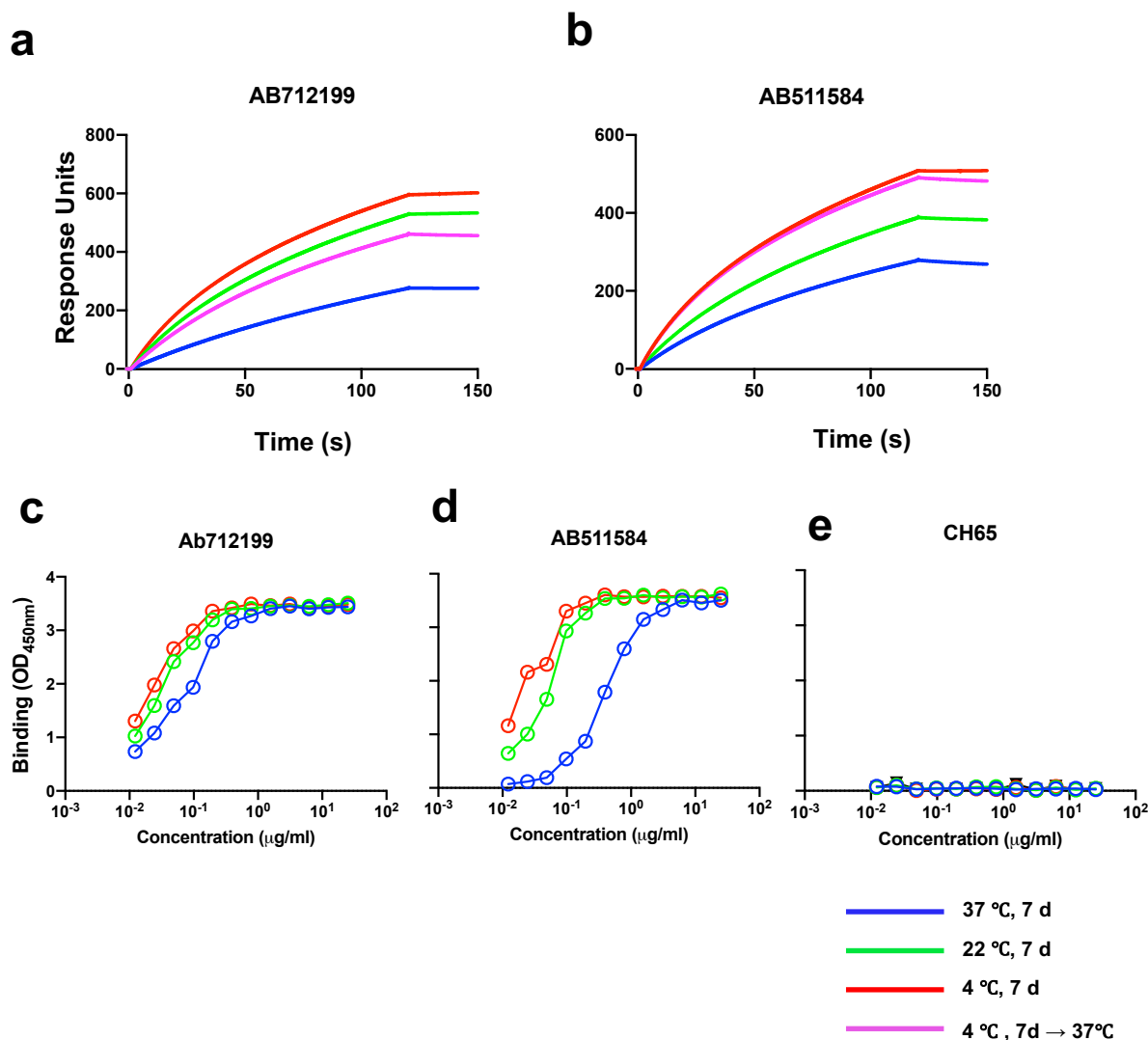
Extended Data Figure 5. Antigenic response of SARS-CoV-2 S ectodomain incubated at different temperatures to antibodies elicited from convalescent patient sera. (a-b) SPR binding profiles showing binding of **(a)** RBD-directed antibody, AB712199, **(b)** S2-directed antibody, AB511584 to spike samples incubated for 1 week at either 37 °C (blue), 22 °C (green) or 4 °C (red). Binding to spike sample first incubated at 4 °C for 1 week, then moved to 37 °C for 3 hours prior to the experiment is shown in magenta. **(c-e)** ELISA binding profiles showing binding of **(c)** RBD-directed antibody, AB712199, **(d)** S2-directed antibody, AB511584, or **(e)** influenza HA-directed antibody CH65 (control) to spike samples incubated for 1 week at either 37 °C (blue), 22 °C (green) or 4 °C (red).
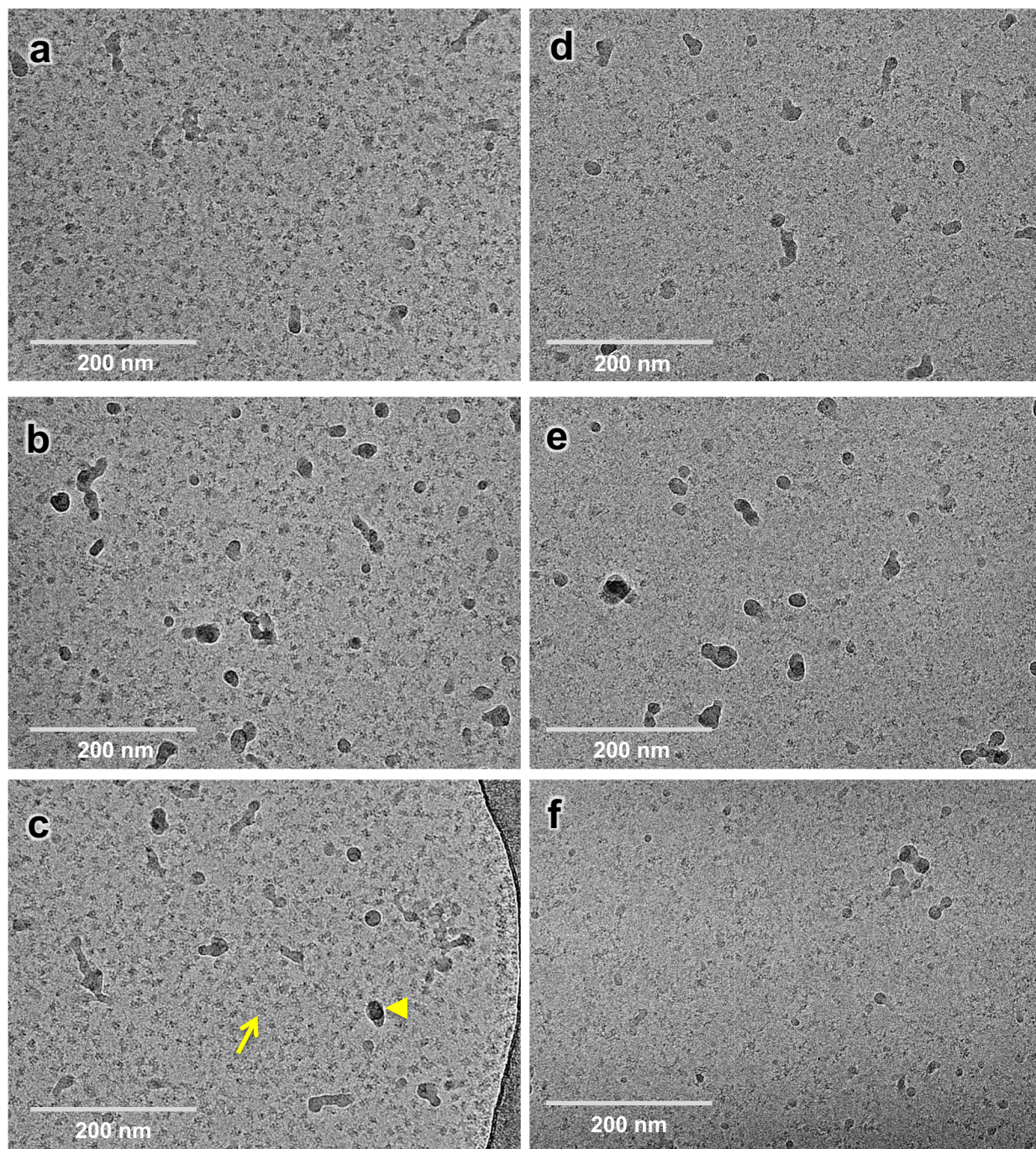
Extended Data Figure 6. Effect of SARS-CoV-2 ectodomain spike sample storage on cryo-EM specimen preparation. (**a-c**) Representative cryo-EM micrographs of a SARS-CoV-2 S ectodomain sample that was flash frozen immediately after purification and stored in -80 °C, then thawed rapidly and incubated for ~ 5 min at 37 °C immediately prior to grid preparation. Cryo-EM images are low contrast, and the desired spike particles appear as medium gray spots (*e.g.* arrow) on a light gray background. Dark gray or black spots are slight ice contamination (*e.g* arrowhead). These panels on the left show an excellent distribution of discrete spike particles. (**d-f**) Representative cryo-EM micrographs of SARS-CoV-2 S ectodomain samples that were stored for ~1 week at 4 °C prior to grid preparation. Compared to the panels of the left, these panels on the right show a sparse field-of-view with very few intact spike particles visible. A similar spike concentration (~1 mg/ml) was used to freeze all the samples. Micrographs were collected on a Titan Krios microscope with a Gatan K3 camera.
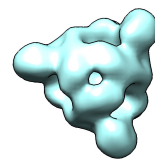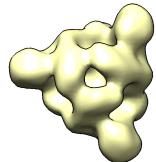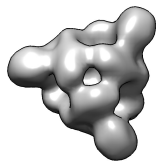
a
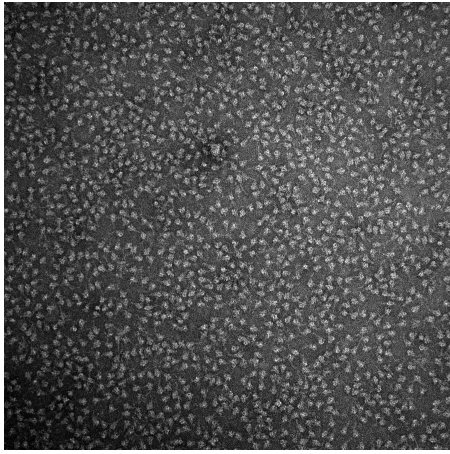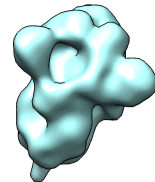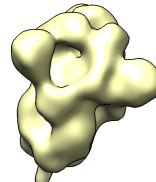
200nm

b
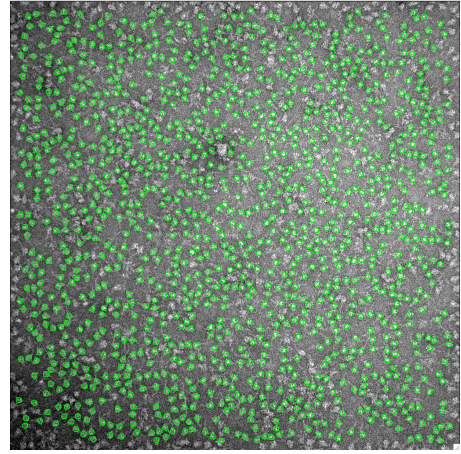
c
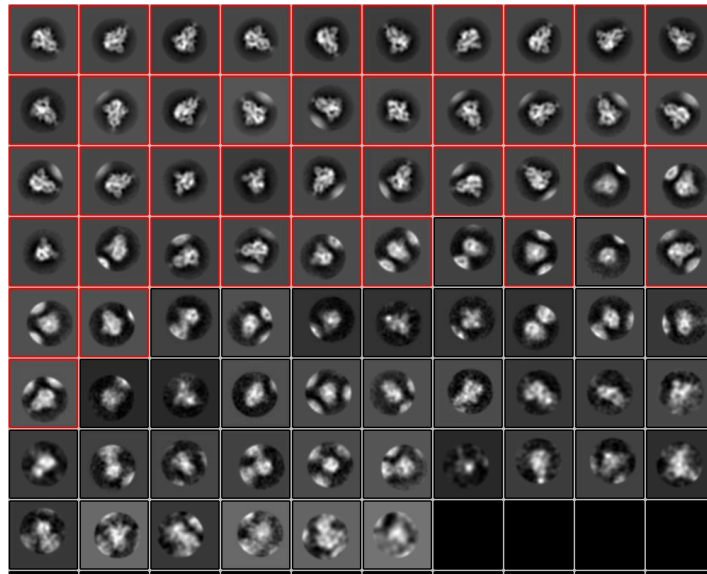
d

Class 1   Class 2   Class 3

100% "down"

50 Å

Extended Data Figure 7. NSEM workflow for rS2d-HexaPro. (a) Representative NSEM micrograph **(b)** Representative NSEM micrograph showing particle picks in green **(c)** 2D class averages; the particles in the classes marked with a red box were taken forward to the next steps on the analysis **(d)** 3D classes showing top views in the top row and side views in the bottom row. 30,000 particles were used for 3D classification. These were separated into 3 3D classes that were reconstructed using C1 symmetry. Only all-RBD-down classes were observed. Also see Supplementary Movie S1 that shows the residual movement in the RBDs despite being locked down by a RBD-to-S2 disulfide.

Supplementary Table 1. Thermostability of the SARS-CoV-2 spike ectodomain stored at different temperatures measured by DSF. Inflection temperatures from DSF plots shown in Figure 1F, expressed as averages ± standard deviation, N=5.

Storage Temperature	T^i_1	T^i_2	T^i_3
37 °C	53.7 ± 1.1	65 ± 0.2	74.8 ± 0.2
22 °C	49.9 ± 0.2	58.6 ± 0.3	74.2 ± 0.2
4 °C	49.9 ± 0.4	57.5 ± 0.3	71.9 ± 0.2
4->37 °C Recovery	52.2 ± 0.5	58.8 ± 0.5	74.1 ± 0.3

Supplementary Table 2. Thermostability of the SARS-CoV-2 spike ectodomain stored at different temperatures measured by DSC. Table of melting temperatures, T_m, with values expressed as mean ± range, N=2.

| Storage Temp.	Transition Peak 1 T_m (°C)	Transition Peak 2 T_m (°C)
37 °C	N/A	65.5 ± 0.2
22 °C	48.2 ± 0.1	65.8 ± 0.1
4 °C	48.41 ± 0.01	65.1 ± 0.3
4 → 37 °C Recovery	49.2 ± 0.1	65.95 ± 0.02
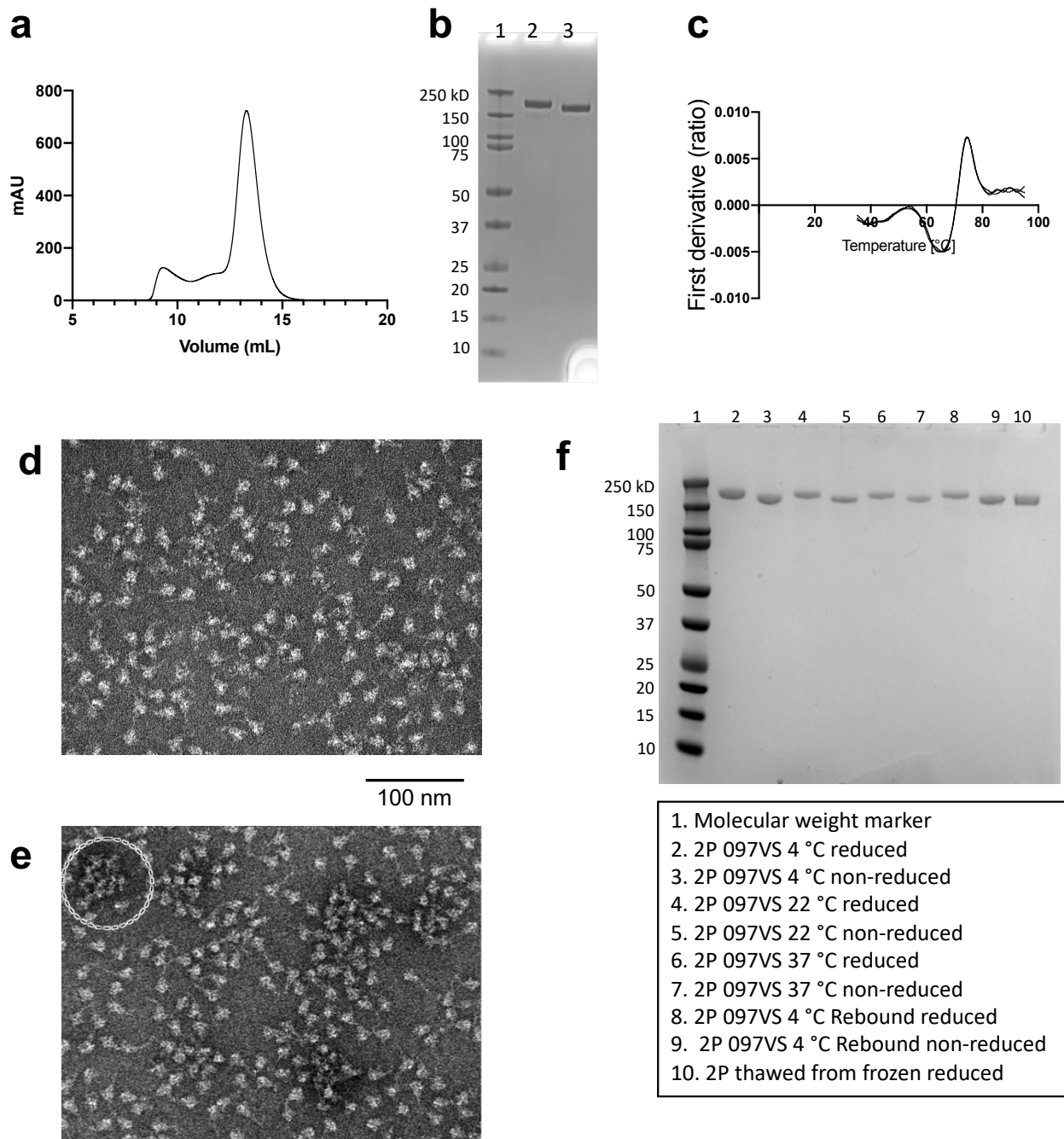
Supplementary Figure 1. SDS-PAGE and NSEM analysis of spike proteins incubated at different temperatures. (a) SEC profile, **(b)** SDS-PAGE analysis (lane 1= molecular weight marker, lane 2= reducing conditions, lane 3= non-reducing conditions) and **(c)** DSF profile of a freshly purified sample of the 2P spike. **(d)** NSEM micrograph of 2P spike after storage at 22 °C for one week. **(e)** NSEM micrograph of 2P spike after storage at 4 °C for one week followed by recovery at 37 °C for 6 days. The circle indicates spike aggregation visible in the micrograph. **(f)** SDS-PAGE analysis of the 2P spike incubated at different temperatures. The legend under the gel lists the sample loaded in each lane. The sample description follows this order- construct name (e.g. 2P), lot # (e.g. 097VS), temperature at which sample was incubated for 1 week (e.g. 4 °C). Samples that were incubated first for 1 week at 4 °C, then moved to 37 °C are labeled as "Rebound". Reduced and non-reduced sampled are noted. 3 µg sample was loaded in each well.
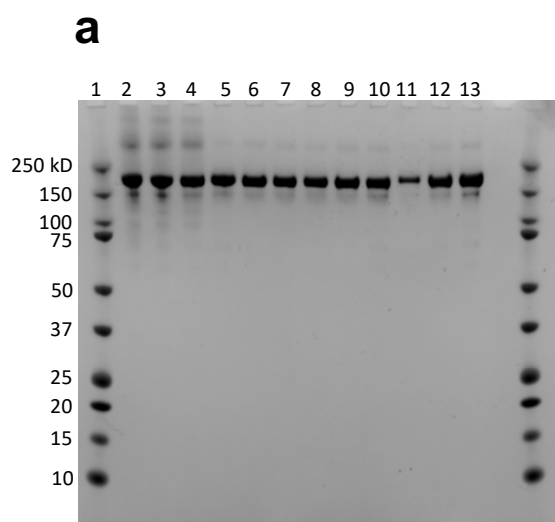
a

| | 1 | 2 | 3 | 4 | 5 | 6 | 7 | 8 | 9 | 10 | 11 | 12 | 13 |

250 kD
150
100
75
50
37
25
20
15
10

Reduced

1. Molecular weight marker
2. 2P-N165A 095VS 37 °C
3. 2P-N234A 096VS 37 °C Repeat 1
4. 2P-N234A 096VS 37 °C Repeat 2
5. 2P-N165A 095VS 4 °C
6. 2P-N234A 096VS 4 °C Repeat 1
7. 2P-N234A 096VS 4 °C Repeat 2
8. 2P-N165A 095VS 22 °C
9. 2P-N234A 096VS 22 °C Repeat 1
10. 2P-N234A 096VS 22 °C Repeat 2
11. 2P-N165A 095VS 4 °C Rebound
12. 2P-N234A 096VS 4 °C Rebound Repeat 1
13. 2P-N234A 096VS 4 °C Rebound Repeat 2

b

| | 1 | 2 | 3 | 4 | 5 | 6 | 7 | 8 | 9 | 10 | 11 | 12 | 13 | 14 |

250 kD
150
100
75
50
37
25
20
15
10
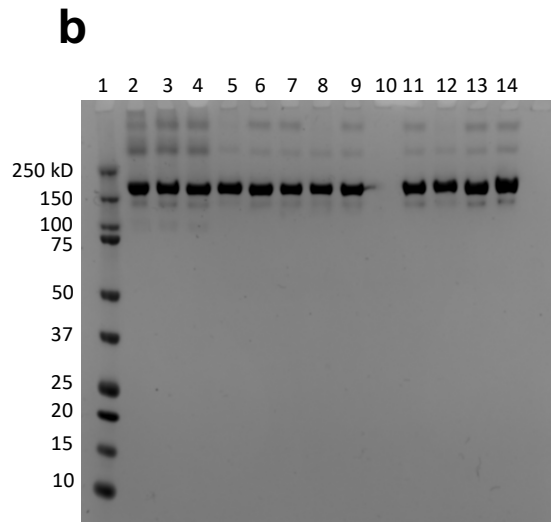
Non-Reduced

1. Molecular weight marker
2. 2P-N165A 095VS 37 °C
3. 2P-N234A 096VS 37 °C Repeat 1
4. 2P-N234A 096VS 37 °C Repeat 2
5. 2P-N165A 095VS 22 °C
6. 2P-N234A 096VS 4 °C Repeat 1
7. 2P-N234A 096VS 4 °C Repeat 2
8. 2P-N165A 095VS 22 °C
9. 2P-N234A 096VS 22 °C Repeat 1
10. Intentionally left blank
11. 2P-N234A 096VS 22 °C Repeat 2
12. 2P-N165A 095VS 4 °C Rebound
13. 2P-N234A 096VS 4 °C Rebound Repeat 1
14. 2P-N234A 096VS 4 °C Rebound Repeat 2

Supplementary Figure 1 (contd). SDS-PAGE analysis of spike proteins incubated at different temperatures. (a) SDS-PAGE under reducing conditions and **(b)** SDS-PAGE under non-reducing conditions. The legend below each gel lists the sample loaded in each lane. The sample description follows this order- construct name (e.g. 2P-N165A), lot # (e.g. 095VS), temperature at which sample was incubated for 1 week (e.g. 4 °C). Samples that were incubated first for 1 week at 4 °C, then moved to 37 °C hours are labeled as "Rebound". 3 µg sample was loaded in each well.

Left gel legend:
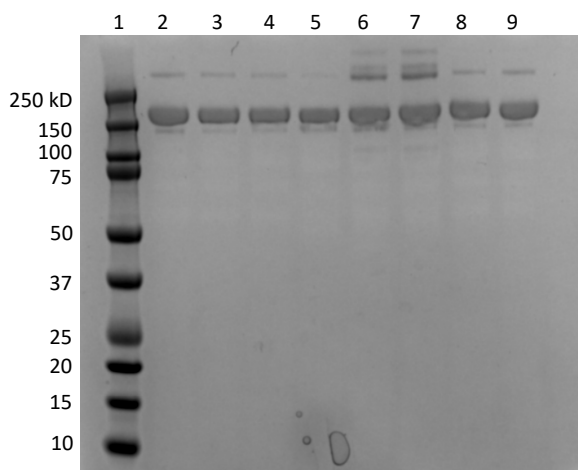
1. Molecular weight marker
2. Hexapro 111KJ 4 °C Repeat 1
3. Hexapro 111KJ 4 °C Repeat 2
4. Hexapro 111KJ 22 °C Repeat 1
5. Hexapro 111KJ 22 °C Repeat 2
6. Hexapro 111KJ 37 °C Repeat 1
7. Hexapro 111KJ 37 °C Repeat 2
8. Hexapro 111KJ 4 °C Rebound Repeat 1
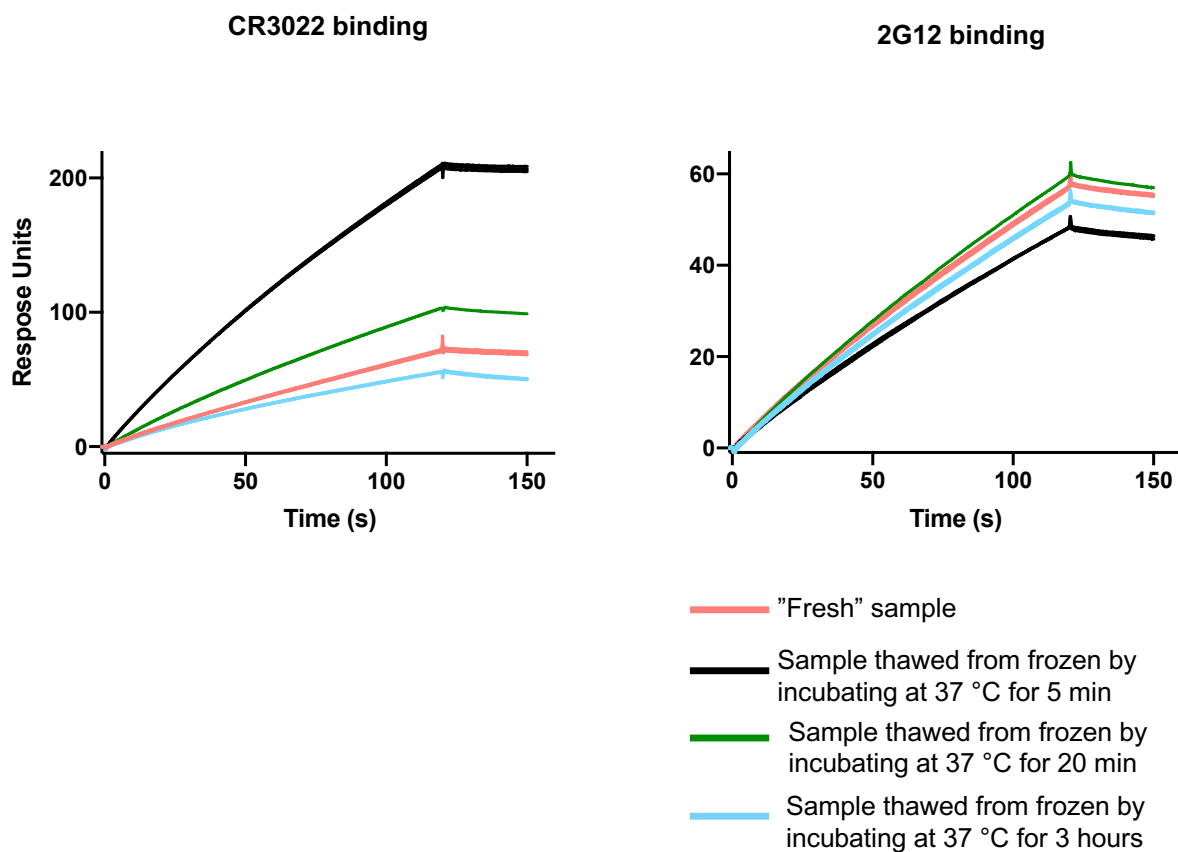9. Hexapro 111KJ 4 °C Rebound Repeat 2

Right gel legend:
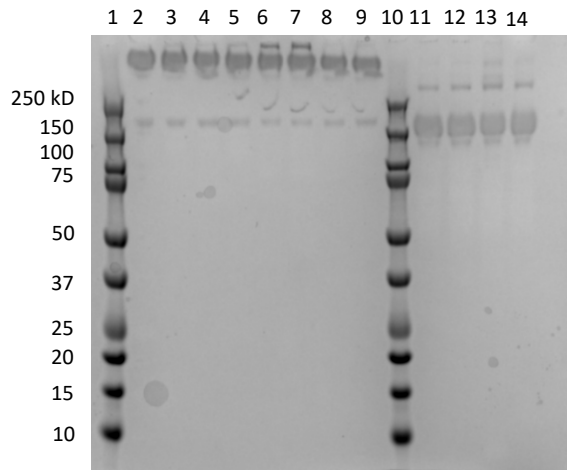
1. Molecular weight marker
2. rS2d-Hexapro 126KJ 4 °C Repeat 1
3. rS2d-Hexapro 126KJ 4 °C Repeat 2
4. rS2d-Hexapro 126KJ 22 °C Repeat 1
5. rS2d-Hexapro 126KJ 22 °C Repeat 2
6. rS2d-Hexapro 126KJ 37 °C Repeat 1
7. rS2d-Hexapro 126KJ 37 °C Repeat 1
8. rS2d-Hexapro 126KJ 4 °C Rebound Repeat 1
9. rS2d-Hexapro 126KJ 4 °C Rebound Repeat 2
10. Molecular weight marker
11. 2P 025MFK 4 °C
12. 2P 025MFK 22 °C
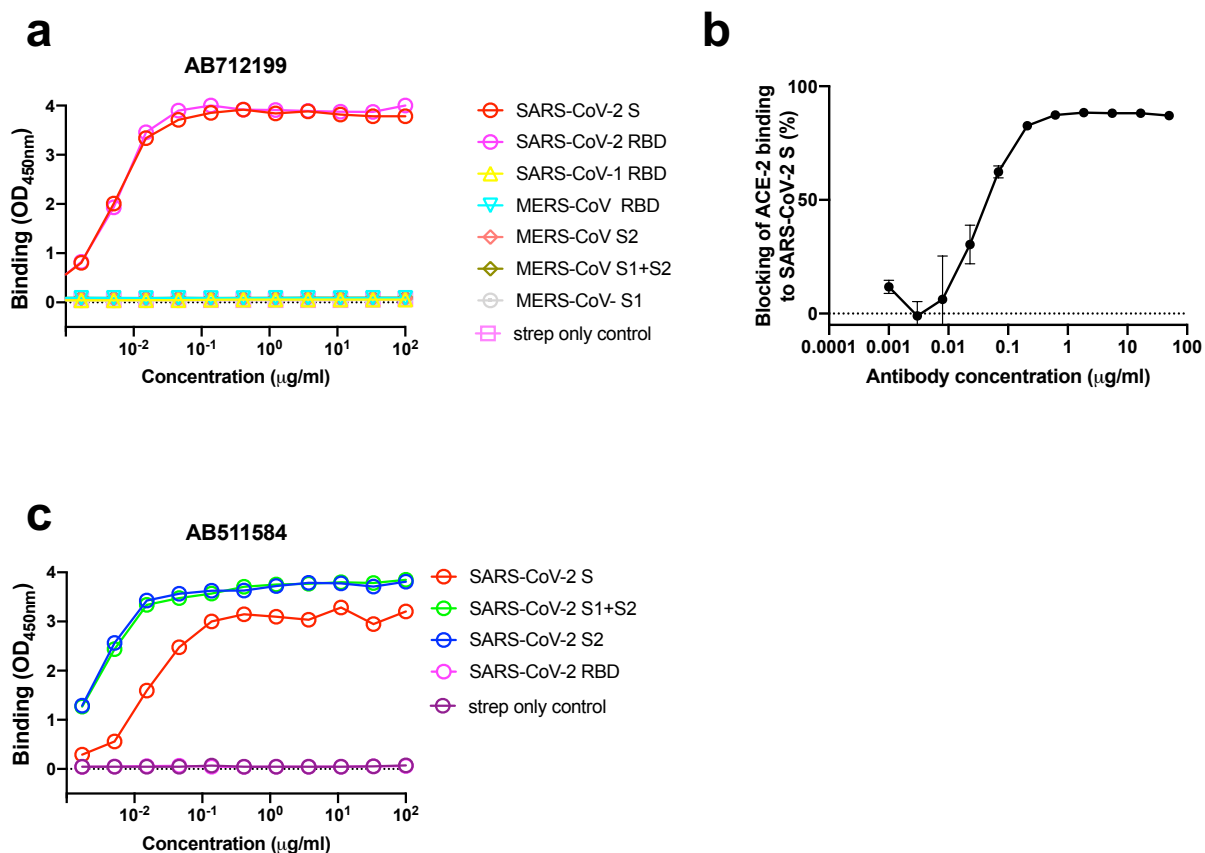13. 2P 025MFK 37 °C
14. 2P 025MFK 4 °C Rebound

Supplementary Figure 1 (contd). SDS-PAGE analysis of spike proteins incubated at different temperatures. SDS-PAGE under non-reducing conditions. The legend below each gel lists the sample loaded in each lane. The sample description follows this order- construct name (e.g. Hexapro), lot # (e.g. 111KJ), temperature at which sample was incubated for 1 week (e.g. 4 °C). Samples that were incubated first for 1 week at 4 °C, then moved to 37 °C are labeled as "Rebound". 10 μg sample was loaded in each well.

CR3022 binding

2G12 binding

Lot# 097VS

Lot# 025MFK

37 ℃, 7 d
22 ℃, 7 d
4 ℃, 7 d
4 ℃ , 7d → 37℃
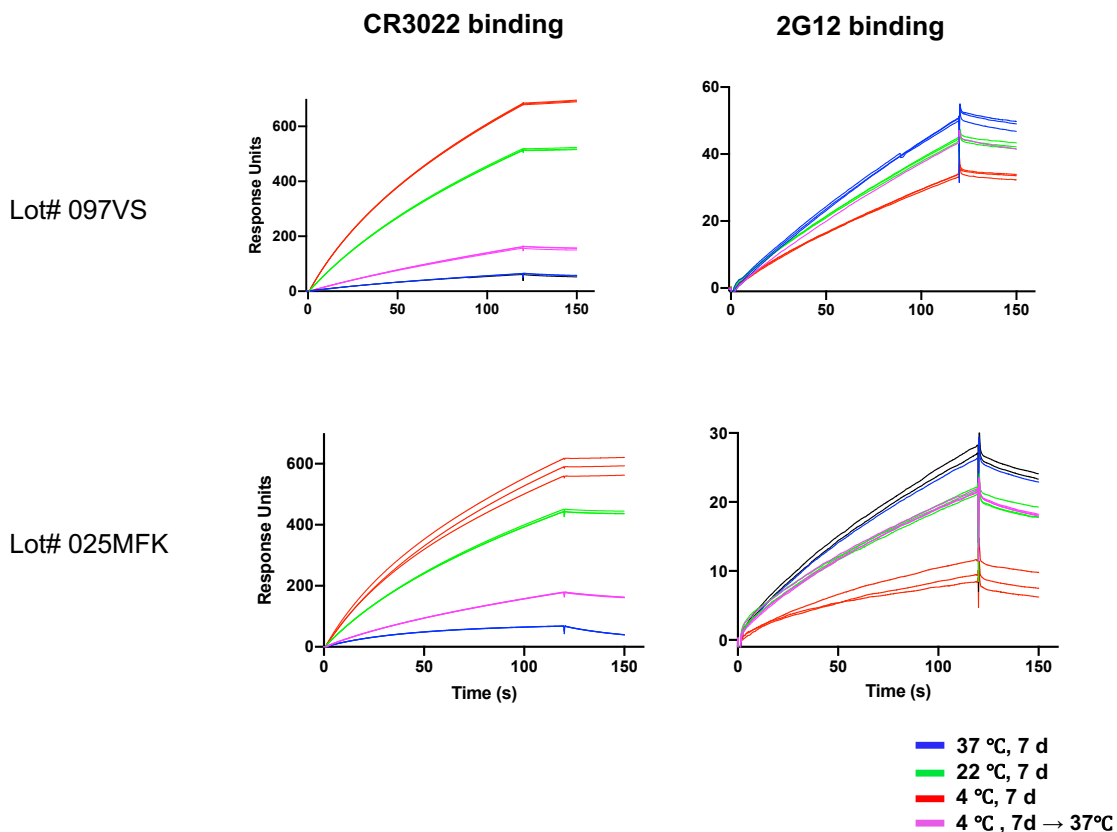
Supplementary Figure 2. Effect of storage temperature on 2P spike antigenicity measured with two different protein lots. Antibody CR3022 IgG (left) and 2G12 IgG (right) binding to spike stored at different temperatures measured by SPR. Data for spike samples measured after a 1-week incubation at 37, 22, and 4 °C, are shown in blue, green, and red respectively; sample stored 1 week at 4 °C and then incubated for 6 hours at 37 °C shown in magenta. During the SPR run the sample chamber was maintained at temperatures of 37 °C, 22 °C and 8 °C, for the 37 °C, 22 °C and 4 °C incubated samples, respectively. The binding experiments were carried out at 25 °C.

CR3022 binding

2G12 binding

Response Units vs Time (s)

Legend:
- "Fresh" sample
- Sample thawed from frozen by incubating at 37 °C for 5 min
- Sample thawed from frozen by incubating at 37 °C for 20 min
- Sample thawed from frozen by incubating at 37 °C for 3 hours

Supplementary Figure 3. CR3022 and 2G12 binding to freshly purified spike and spike that has been flash frozen then thawed. Antibody CR3022 IgG (left) and 2G12 IgG (right) binding to spike that was either freshly purified or flash-frozen in liquid N2, then thawed by incubating at 37 °C for different periods of time.
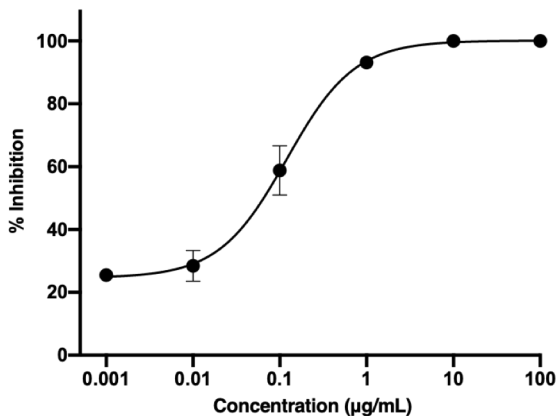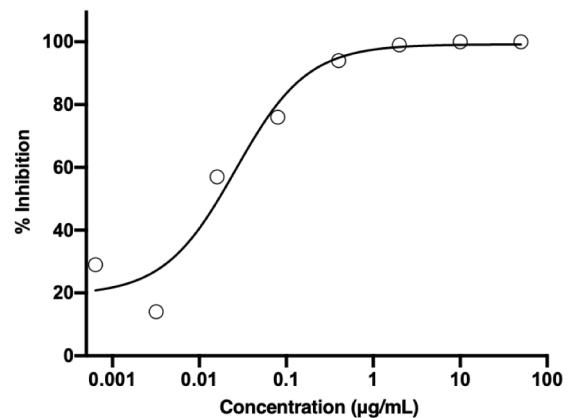
a AB712199

Legend:
- SARS-CoV-2 S
- SARS-CoV-2 RBD
- SARS-CoV-1 RBD
- MERS-CoV RBD
- MERS-CoV S2
- MERS-CoV S1+S2
- MERS-CoV- S1
- strep only control

b

c AB511584

Legend:
- SARS-CoV-2 S
- SARS-CoV-2 S1+S2
- SARS-CoV-2 S2
- SARS-CoV-2 RBD
- strep only control

d

	SARS-CoV-2 Spike/2p	SARS-CoV-2 RBD	SARS-CoV-2 S2
AB511584	11.59	0	16.11
AB712199	16.705	17.048	0

Supplementary Figure 4. Characterization antibodies isolated from COVID-19 convalescent donors by ELISA (**a**) Epitope mapping of antibody AB712199 shows that the antibody binds the SARS-CoV-2 RBD region, (**b**) Blocking of ACE-2 binding to SARS-CoV-2 S ectodomain by AB712199, **(c)** Epitope mapping of antibody AB511584 shows that the antibody binds the SARS-CoV-2 S2 region **(d)** Summary of epitope mapping from ELISA showing log of the area under the curves.

a

	Microneutralization assay	Pseudovirus assay		PRNT		
	Geometric Mean Effective conc. (µg/ml)	IC50 (µg/ml)	IC80 (µg/ml)	IC50 (µg/ml)	IC80 (µg/ml)	IC90 (µg/ml)
Ab511584	>100	NA	NA	NA	NA	NA
Ab712199	0.55	0.012	0.11	0.316	0.120	0.863

b

c

Supplementary Figure 5. Characterization antibodies isolated from COVID-19 convalescent donors in neutralization assays. (**a**) Summary of neutralization profiles of antibodies AB511584 and AB712199 by three different assays. (**b**) Neutralization of SASR-CoV-2 by AB712199 measured using plaque reduction neutralization test. **(c)** Neutralization of SASR-CoV-2 by AB712199 measured using a pseudovirus assay.